Journal of Mammalian Evolution
https://doi.org/10.1007/s10914-022-09600-0

ORIGINAL PAPER

Middle Pleistocene Steppe Lion Remains from Grotte de la Carrière (Têt Valley, Eastern Pyrenees)

Maria Prat-Vericat[1] · Adrian Marciszak[2] · Isaac Rufí[3] · Leonardo Sorbelli[1] · Manel Llenas[1,4,5] · Saverio Bartolini Lucenti[6,7] · Joan Madurell-Malapeira[1,4,5]

Accepted: 7 January 2022

Abstract
Late Pleistocene cave lions are one of the most iconic species of Northern Hemisphere Quaternary taphocoenoses. Despite their often-scarce record in cave environments, their ubiquitous distribution across Eurasia and North America assemblages attests to their position as top ice-age predators. Nevertheless, the origins of these former large felids, their distribution during the Middle Pleistocene, and their paleoecology during co-existence with the scimitar-toothed cat *Homotherium* remain debated. Here we describe for the first time an abundant collection of large-sized and stout felid remains from the recently discovered site of Grotte de la Carrière in Eastern Pyrenees, with an estimated age corresponding to MIS 9. Our results highlight the larger size of Middle Pleistocene lions compared to Late Pleistocene ones as well as a trend of decreasing in size, which has been previously stated by other authors. Grotte de la Carrière steppe lions have similar morphological and biometrical parameters to those of other samples from MIS 11–9, being larger and stouter than younger latest Middle Pleistocene-Late Pleistocene forms and slightly smaller than older MIS 15–12 forms.

Keywords Pleistocene · Quaternary · Pyrenees · Carnivore · Felidae · *Panthera fossilis*

Introduction

The Earliest Lions and their European Record

Nowadays, the African lion (*Panthera leo*) lives mainly in scattered populations across Sub-Saharan Africa (Stuart and Lister 2011; Bellani 2020). However, Middle to Late Pleistocene lions were one of the most widely distributed terrestrial carnivores (Kahlke 1999; Barnett et al. 2009; Stuart and Lister 2011; Bellani 2020), being recorded in Europe, Asia, and North America in the Late Pleistocene under different *Panthera* specific attributions, such as *Panthera spelaea*, *P. fossilis, P. intermedia,* and *P. atrox*. Since the split of their ancestors in eastern Africa, which has been dated to the earliest Early Pleistocene (ca. 2.5 Ma) (Werdelin and Lewis 2005; Argant et al. 2007; Sabol 2011), lions spread over the Holarctic domain, where they became one of the top predators of the European carnivore guild (Turner 2009; Lewis et al. 2010; Bocherens et al. 2011). They survived until the early Holocene, when the last cave lion lineage went extinct ca. 12 ka (Stuart and Lister 2011).

✉ Joan Madurell-Malapeira
joan.madurell@icp.cat

1 Institut Català de Paleontologia Miquel Crusafont, Universitat Autònoma de Barcelona, Edifici ICTA-ICP, C/ de Les Columnes S/N Campus de La UAB, Cerdanyola del Vallès, 08193 Barcelona, Spain

2 Department of Paleozoology, Faculty of Biological Sciences, University of Wrocław, Sienkiewicza 21, 50-335 Wrocław, Poland

3 Departament d'Història i Història de l'Art, Universitat de Girona, Pl. Ferrater Mora, 1, 17004 Girona, Spain

4 Secció Villalta, Federació Catalana d'Espeleologia, c\ del Mas Casanovas 66, 08025 Barcelona, Spain

5 Conflent Spéléo Club, 4, Traverse Des Fabriques, 66500 Prades de Conflent, France

6 Dipartimento Di Scienze Della Terra, Università Di Firenze, Via G. La Pira 4, 50121 Firenze, Italy

7 Museo Di Storia Naturale, Università Degli Studi Di Firenze, Via la Pira, 50121 Firenze, Italy

Published online: 14 March 2022

Historically, the Middle Pleistocene lion fossil record is not as well-known as the Late Pleistocene one due to the scarcity of Middle Pleistocene sites. Sites have mainly been known in Southern and Central Europe (Fig. 1) such as Breccia de Château (Argant 1988) and Mauer and Mosbach (Schütt and Hemmer 1978). This scantiness does not help clarify the evolutionary history of Pleistocene lions. The first documented Eurasian lions come from Pakefield (ca. 750 ka; Lewis et al. 2010), Kozi Grzbiet (ca. 750 ka; Marciszak et al. 2021), and Isernia la Pineta (ca. 650 ka; Sala 1990). Recent paleontological works have pointed to eastern Africa as the origin of lion dispersion around 800 ka (Argant 1991; Burger et al. 2004; Argant et al. 2007; Sabol 2011). However, the presence of lions in the latest Early Pleistocene of Iberia (i.e., Vallparadís Section and Cueva Victoria, Spain) suggests that the complex history of European lions may have started earlier (Madurell-Malapeira et al. 2014, 2017). Furthermore, an entrance from Western Siberia should not be ruled out, as Sotnikova and Foronova (2014) recently described *P. fossilis* in the Kuznetsk Basin (Russia) at ca. 1.0 Ma.

Unfortunately, the taxonomy of the cave lion lineage still generates debate in the scientific community (Sabol 2011; Marciszak et al. 2014). According to some authors, skull similarities with modern lions indicate that the Pleistocene forms are a large extinct subspecies of *P. leo* (Ballesio 1975, 1980; Turner 1984). In contrast, others support the existence of two valid chronospecies: *Panthera fossilis* (von Reichenau, 1906) and *Panthera spelaea* (Goldfuss, 1810) (Sotnikova and Nikolskiy 2006; Sabol 2014; Barnett et al. 2016). Other scholars regard both of these species as subspecies of *P. spelaea* (Argant et al. 2007; Barycka 2008; Marciszak and Stefaniak 2010). Recent DNA studies reveal that the cave lion putatively dispersed over Europe ca. 600 ka after becoming isolated from Asian and African populations (Burger et al. 2004; Barnett et al. 2009) and diverged from modern lions around 1.89 Ma (Barnett et al. 2016), becoming a clear monophyletic outgroup (Barnett et al. 2016; deManuel et al. 2020). Other more recent studies have supported the existence of three different clades of cave lions that diverged from extant species ca. 1.85 Ma. One of these clades was putatively restricted to Beringia, while others were prevalent in Eurasia (Stanton et al. 2021).

Despite everything, it seems to be clear that *P. fossilis* spread to Central and Eastern Europe and dispersed across mountain areas during marine isotopic stages (MIS) 17–12 (Sabol 2011), dominating them until MIS 10–9. Then, *P. fossilis* was progressively replaced by *P. spelaea* (Argant 2010; Baryshnikov and Tsoukala 2010; Marciszak et al. 2014). According to Marciszak and Stefaniak (2010), the replacement occurred around MIS 7-5e. However, fossil specimens of lions belonging to MIS 9–6 present intermediate characteristics (Marciszak et al. 2014; Argant and Brugal 2017). Argant and Brugal (2017) identify the fossil record from Igue-de-Rameaux (MIS 9–7) as *P. l. intermedia*.

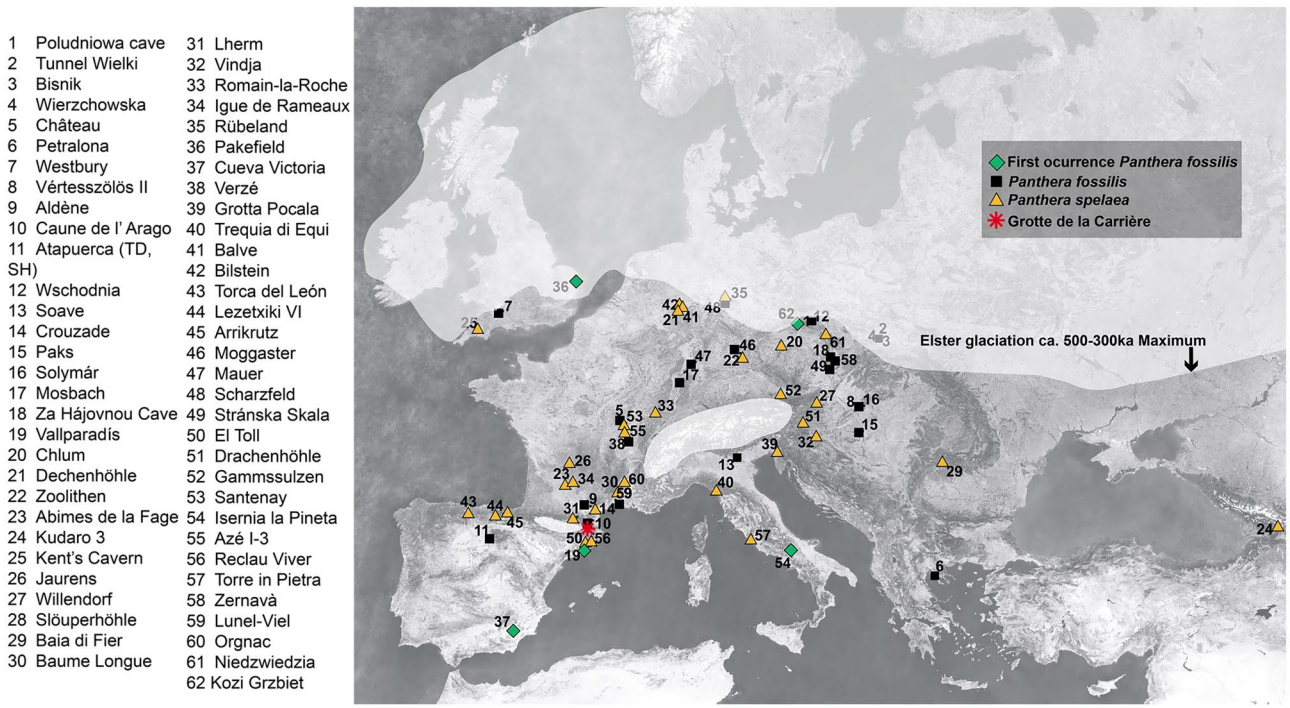

Fig. 1 Grotte de la Carrière geographical location and European distribution of Middle and Late Pleistocene fossiliferous sites mentioned in the text

Nevertheless, as indicated by European regional differences, the replacement probably occurred during a different span of time.

All these phylogenetic problems are partly a consequence of the high adaptability of European lions to diverse environmental conditions and biomes (Sabol et al. 2018). Following this interpretation, it seems plausible that *P. fossilis* was distributed throughout European lands (Fig. 1), inhabiting a great variety of biotopes, from open lowlands and woodlands to mountainous boreal forest (Turner 2009; Baryshnikov 2011; Sabol et al. 2018). Their large size qualifies them to be predators of a wide prey spectrum, including large-sized herbivores and occasionally cave bears (Hemmer 2004; Baryshnikov 2011; Bocherens et al. 2011; Diedrich 2011; Stuart and Lister 2011; van Valkenburgh et al. 2016). In general, regional differences attributed to habitat and prey availability, in addition to sexual dimorphism and the scantiness of fossil record, constrain attempts to correctly resolve phylogenetic relationships (Schütt 1969; Turner 1984; Argant et al. 2007; Diedrich 2011; Christiansen and Harris 2012; Marciszak et al. 2014, 2017; Sabol et al. 2018).

The field surveys performed the last five years in the newly discovered site of Grotte de la Carrière inside the Reséau Lachambre (Têt Valley, Eastern Pyrenees) have provided new Middle Pleistocene lion material chronologically constrained to MIS 9 (Fig. 2) and previously tentatively attributed to *P. fossilis* (Madurell-Malapeira and Llenas 2018, 2019; Prat-Vericat et al. 2019, 2020). The aim of the present paper is to provide a detailed description of all unearthed specimens, determine their morphological and taxonomical position close to the latest known occurrences of *P. fossilis,* and report new knowledge about the paleobiology of this European Lion.

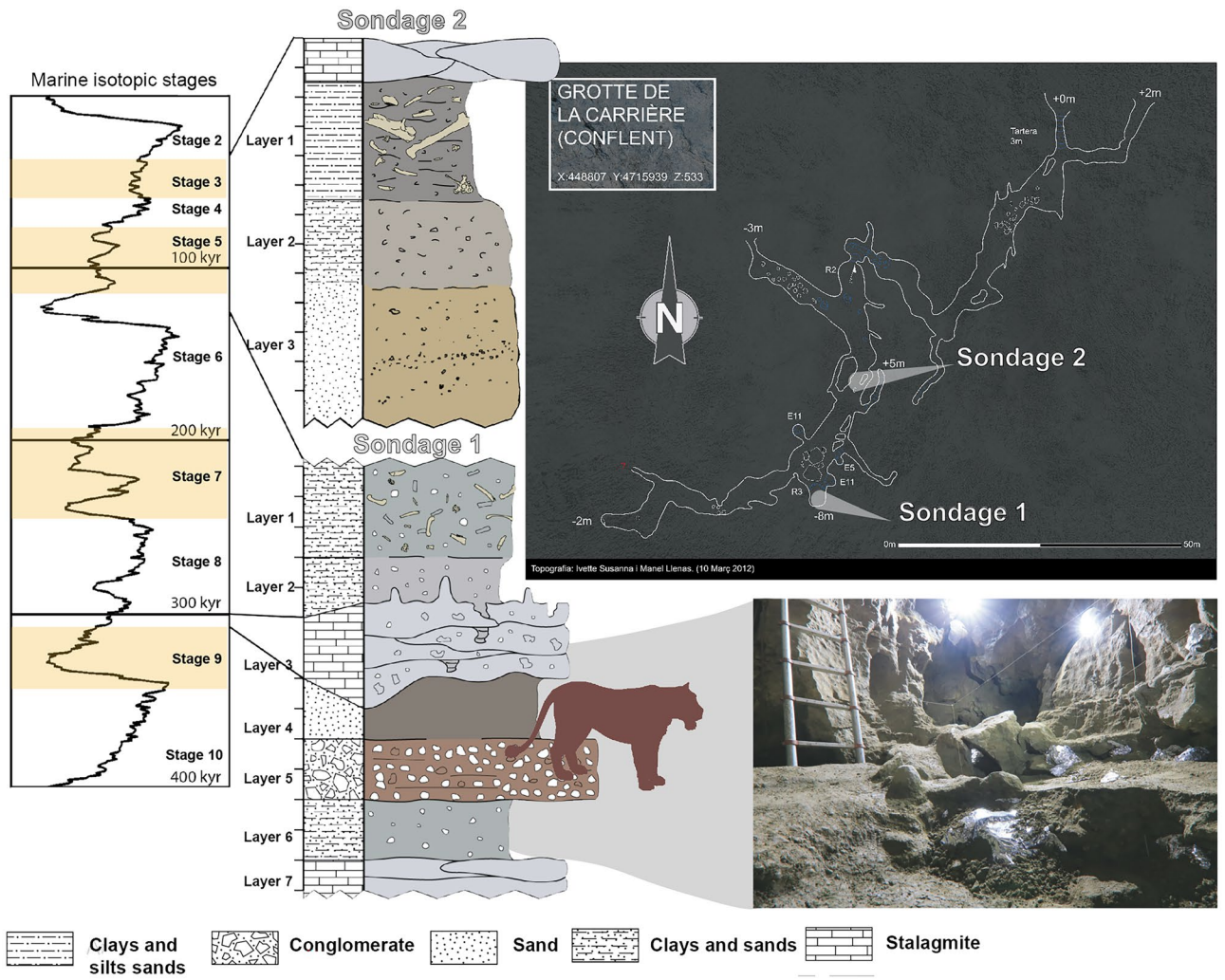

Fig. 2 Grotte de la Carrière topography, stratigraphy, and chronology of Sondage 1 and 2. Below on the right shows a picture of Sondage 1 layer 4 squares C6 and C5 in the 2020 field season

Les Gorges de Villefranche and the Réseau Lachambre

Les Gorges de Villefranche are an important karst system in the Têt Valley (Eastern Pyrenees, France) composed of three large cave networks located in the surroundings of the Villefranche-de-Conflent village: R. d'en Gorner, R. de Fullà-Canaletes, and R. Lachambre (Madurell-Malapeira et al. 2019). Since 2011, the paleontological richness from the three karstic systems was highlighted by Federació Catalana d'Espeologia (FCE) and Institut Català de Paleontologia Miquel Crusafont (ICP) in a project led by M. Ll. and J. M.-M., also members of the Conflent Spéléo Club de Prades. The surveys provided an exceptional quantity of paleontological material from different caves that is chronologically constrained from the Middle to the Late Pleistocene (Madurell-Malapeira et al. 2015).

The Reséau Lachambre, located in the surroundings of Villefranche-de-Conflent village, is a karstic system with more than 25 km of galleries and several accessory cavities (Madurell-Malapeira and Llenas 2018). In one of its accessory caves, namely Grotte de la Carrière, five systematic excavations recovered more than 8,000 well-preserved large mammal remains in two distinct stratigraphic Sondages (Prat-Vericat et al. 2019, 2020).

The cavity located at 540 m of altitude and 75 m above the Lachambre main cave is a Middle to Late Pleistocene cave that was inhabited by the cave bear *Ursus deningeri* in the lower layers (Sondage 1) and *Ursus spelaeus* in Sondage 2 (Madurell-Malapeira and Llenas 2019; Prat-Vericat et al. 2020). According to preliminary data, the lion remains have been found in the lower layers of Sondage 1 (Fig. 2) in association with Middle Pleistocene assemblage (ca. 0.3 Ma; MIS 9; López-García et al. 2016; Madurell-Malapeira and Llenas 2018).

Material and Methods

Material

All the specimens described herein were restored by the preparation lab team of the Institut Català de Paleontologia Miquel Crusafont (ICP, Spain) and are under supervision of the Direction Regionalle des Affaires Culturelles (DRAC) of Occitanie (Montpellier, France) and the Conflent Spéléo Club de Prades and housed in Prades-de-Conflent (Occitaine, France).

The material has been compared to several lion species from Eurasia (*Panthera leo*, *P. spelaea*, *P. fossilis,* and *P. intermedia*) on the basis of published descriptions and measurements (Online Resource 1, Tables S1–S4). The fossil sample has been classified into four paleoclimatic ages according to Alps glacial stages (Fig. 3): Günz (MIS 15–12), Mindel (MIS 11–9), Riss (MIS 8–6), and Würm (MIS 5e-2). This classification follows Marciszak et al. (2021) and has been done to minimize the influence of climatic events and the imprecise dating of old publications on phylogenetic interpretations. The most significant division is MIS 11–9, which spans the mid-Brunhes transition (MBT; ca. 430 ka), when climatic fluctuations could have impacted middle Middle Pleistocene lions' evolutionary trends. Similarly, the Late Pleistocene sample includes several phases of climatic oscillations. Unfortunately, we cannot divide the interval from MIS 5 to MIS 2 because of the lack of fossil records. The sample includes metric data from the fossil sites listed below, which are grouped by age. To avoid confusion, *P. l. intermedia* from Igue-de-Rameaux have been placed with the "*spelaea*" group.

Middle Middle Pleistocene (MIS 15–12; 712–424 ka) *P. fossilis*: Tunnel Wielki (Marciszak et al. 2019), Mosbach (Hemmer and Schütt 1970), Breccia de Château (Argant 1991; Argant et al. 2007), Westbury (Bishop 1982), Caune de l'Arago (Testu 2006), Mauer (Hemmer and Schütt 1970), Scharzfeld (= Unicorn cave; Schütt 1969; Hemmer and Schütt 1970) and Stránská Skala (Thenius 1972), Moggaster (Groiss 1992).

Late Middle Pleistocene Steppe Lion (MIS 11–9; 424–300 ka) *P. fossilis*: Moggaster (Groiss 1992), Scharzfeld (= Unicorn cave; Schütt 1969; Hemmer and Schütt 1970), Lunel-Viel (Bonifay 1971), Petralona (Baryshnikov and Tsoukala 2010), Zernavá (Musil 1969), Vértesszölös II (Hankó 2007), Aldène (Testu 2006), Trinchera Dolina TD10-11 (Garcia 2003), Za Hajovnou cave (Sabol 2014), Biśnik Cave (layers 19ad-19) Marciszak and Stefaniak 2010); *P. spelaea*: Orgnac (Testu 2006), Sima de los Huesos (Garcia 2003), Kent's Cavern (Proctor et al. 2005), Torre in Pietra (lower layers; Caloi and Palombo 1978).

Late Middle Pleistocene (MIS 8–6; 300–130 ka) *P. spelaea*: Wierzchowska (Marciszak et al. 2019), Verzé (Bonifay 1971; Testu 2006), Igue-de-Rameaux (=*P. l. intermedia*, Argant and Brugal 2017), Paks (Hankó 2007), Abimes de la Fage (Ballesio 1975), Azé I-3 (Argant 1991), Solymar (Hankó 2007), Lherm (Filhol and Filhol 1871; Testu 2006), Romain-la-Roche (Argant 2010; Guérin et al. 2010), Santenay (Argant 1991).

Late Pleistocene (MIS 5e-2; 130–14 ka) *P. spelaea:* Baume Longue (Bonifay 1971), Jaurens (Ballesio 1980), Rübeland (Baryshnikov 2016), Chlum (Baryshnikov 2016), Willendorf (Thenius 1959), Slöuperhöhle (Zapfe 1966), Baia de Fier (Terzea 1965), Kudaro 1–3 (Baryshnikov and Tsoukala 2010), Zoolithen (Ghezzo 2014; Testu 2006), Equi and Grotta Poccala (Ghezzo 2014), Vindja (Testu 2006), Balve

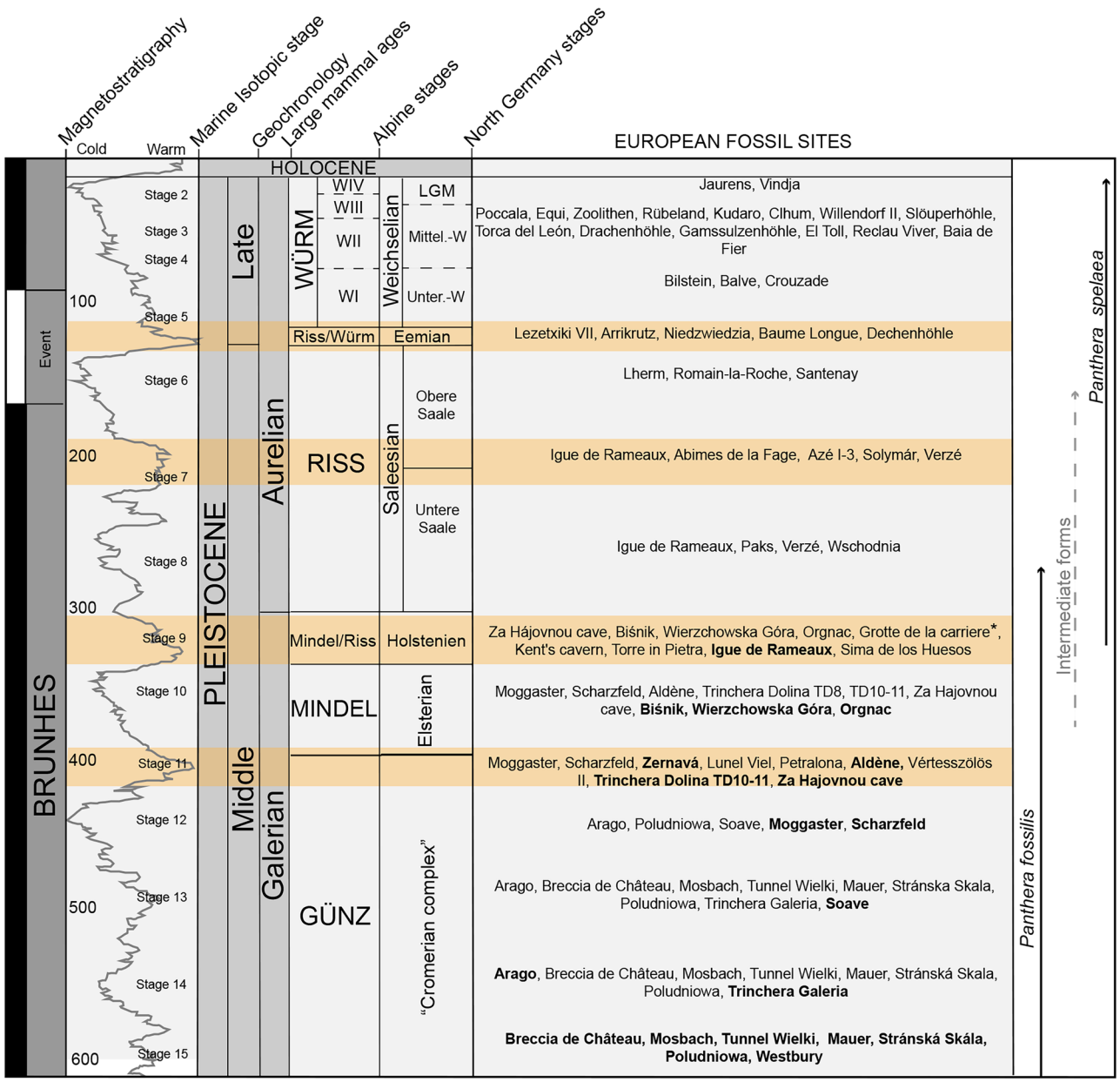

Fig. 3 Biochronological position of the European sites mentioned in the text and the chronological record of *Panthera fossilis* and *Panthera spelaea*. The orange squares mark the relevant Middle Pleistocene interglacials

and Bilstein cave (Diedrich 2011), Torca del Léon (Álvarez-Lao et al. 2020), Lezetxiki VI (Altuna 1972), Arrikrutz (Altuna 1972), Reclau Viver (Crusafont-Pairó and Casajuana 1950).

In addition, measurements of North American Late Pleistocene *P. atrox* from Rancho La Brea (ca. 0.4 ka) housed at the George C. Page Museum (La Brea Tar Pits, Los Angeles, USA) and extant *Panthera leo* from Royal Museum for Central Africa (Tervuren, Belgium) were used for the analysis (Tables S3–S4).

Methods

The statistical approach for the systematic classification of Grotte de la Carrière (GDC) individuals was based on classic morphometric analyses performed from dental morphology and represented by bivariate graphs and boxplot performed in PAST v. 3 (Hemmer et al. 2001). We follow Schmid (1940) for terminology (dental and osteological) and the measurements taken with a digital caliper to the nearest 0.1 mm (Fig. 4; Table 1). To test the normal distribution of the analyzed variables such as the homogeneity

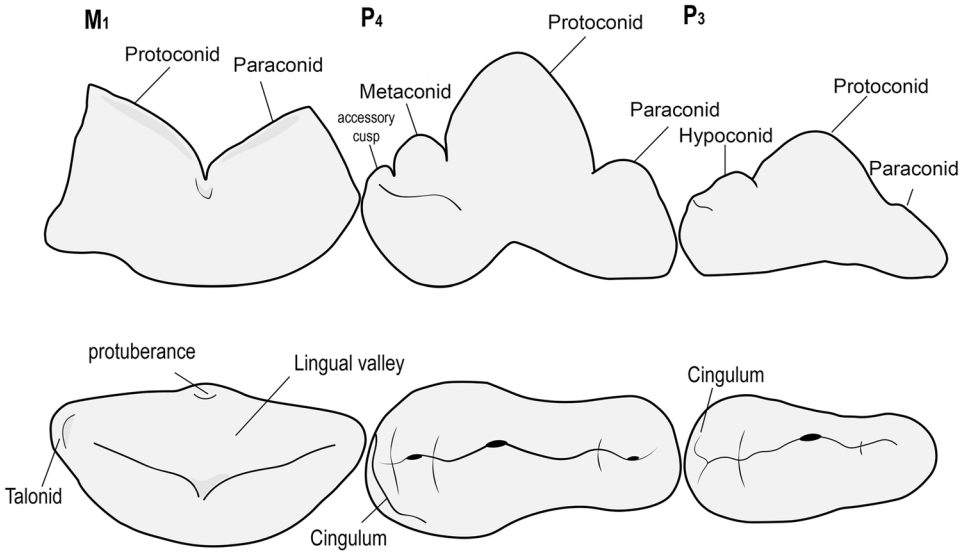

Fig. 4 Morphological parameters for the lower dentition mentioned in the text

of variance across the groups, a Shapiro–Wilk test was carried out on data sets including at least two specimens. Finally, we test the variables that showed significant intergroup differences in a one-way ANOVA (for parametric groups of dental specimens) or Mann–Whitney pairwise (for non-parametric groups of post-cranial specimens). The Mann–Whitney test was run to determinate the statistical relevance for the astragalus (n = 3). Additionally, we tested how several dimensions are affected by sexual dimorphism in various skeletal elements throughout a one-way ANOVA for parametric groups. Finally, we tested the putative climatic and regional differences throughout time

Table 1 Cranial and postcranial measurements in mm of *Panthera fossilis* from Grotte de la Carrière S1. See text for anatomical and measurement abbreviations

Element	Record number	L	W	Lpr	Lpa	Hpr		
p3	GDC2016-D6-225-Nv6	22.7	12.4			12.2		
	GDC2016-B5-29-Nv1	22	12.6					
p4	GDC2016-B4-Nv1	32.5	16.7	14.6				
	GDC2015-Pou-268		16.8	16.9				
m1	GDC2015-Pou-176	30.6	16.3	17.7	16.6			
	GDC2016-D6-64-Nv6	31.7	17.1	18.5	17.4	18.1		
Element	**Record number**	**TL**	**PDap**	**PDtr**	**MDap**	**MDtr**	**DDap**	**DDtr**
Mtc II	GDC-D5-545-Nv4	124.5	37.3	29.5	21.3	20.1	27.5	28.2
	GDC-D6-216-Nv6	117.4	36.9	27.7	21.3	20.7	25.2	25.9
	GDC-D6-137-Nv8	111.3		27.7	20.7	19.7		
Mtc III	GDC-D7-21-Nv4	133.4	34.1	31.3	19.8	18.9		29.1
	GDC-D6-277-Nv6	131.5			19.3	18.2	27.7	28.3
	GDC-D6-276-Nv8	131.9	34.7		20.7	18.7	27.7	28.3
	GDC-C6-17-Nv4	138.6	35.5	32.0	19	20.8	28.4	28.8
Mtc IV	GDC-D6-79-Nv6	127	26.7					
	GDC2019-C7-147-Nv4	124.5	30.9	25.4	17.2	19.4		
Mtc V	GDC-D6-283-Nv8	106.3	29.6	30.1	18.1	14.8		
Mtt II	GDC-D6-80-Nv4	144.6	39.4	31.6	18.8	24.4		26.8
	GDC2020-C5-11-Nv4	151.7	42.4	31.6	22.5	26.1	27.5	30.0
	GDCD2020-C5-484-Nv4		44	33.1		27.4		
Element	**Record**	**TL**	**MD**					
Astragalus	GDC2015-Pou-63	71.9	56.9					
	GDC-D6-122-Nv8	72.1	62.8					
	GDC-B7-579-Nv4	76.5	67.4					
Calcaneum	GDC-D6-318-Nv6	137.9	87.6					

in all the available fossil sample; however, the number of complete fossil bones coming from each locality is normally low. If we separate in glacial/interglacial stages or by latitude, the sample size is short to assess the results or to be statistically significative. Furthermore, to realize an accurate latitudinal distinction, we must take into consideration also the differences among biomes.

Institutional Abbreviations **ICP**, Institut Català de Paleontologia Miquel Crusafont, Universitat Autònoma de Barcelona, Catalonia, Spain; **RMCA**, Royal Museum for Central Africa, Tervuren, Belgium.

Anatomical Abbreviations **c**, lower canine**; L**, length; **M/n**, upper and lower molar, respectively; **Mtc**, metacarpal; **Mtt**, metatarsal; **Pa**, paraconid; **Ph**, Phalanx; **P/p**, upper and lower premolar, respectively; **Pr**, protoconid; **W**, width.

Measurement Abbreviations **DDap**, anterior–posterior distal diameter; **DDtr**, transversal distal diameter; **MD**, Maximum transversal diameter; **MDap**, middle diaphysis anterior–posterior diameter; **MDtr**, middle diaphysis transversal diameter; **PDap**, anterior–posterior proximal diameter; **PDtr**, transversal proximal diameter; **TL**, Total length.

Systematic Paleontology

Order Carnivora Bowdich (1821)
Family Felidae Gray (1821)
Subfamily Felinae Simpson (1945)
Genus *Panthera* Oken (1816)
Panthera fossilis von Reichenau (1906)
Figures 5, 6, 7 and 8

Referred Material 63 cranial and postcranial elements representing at least three Individuals. See detailed list in Table S5.

Measurements See Table 1

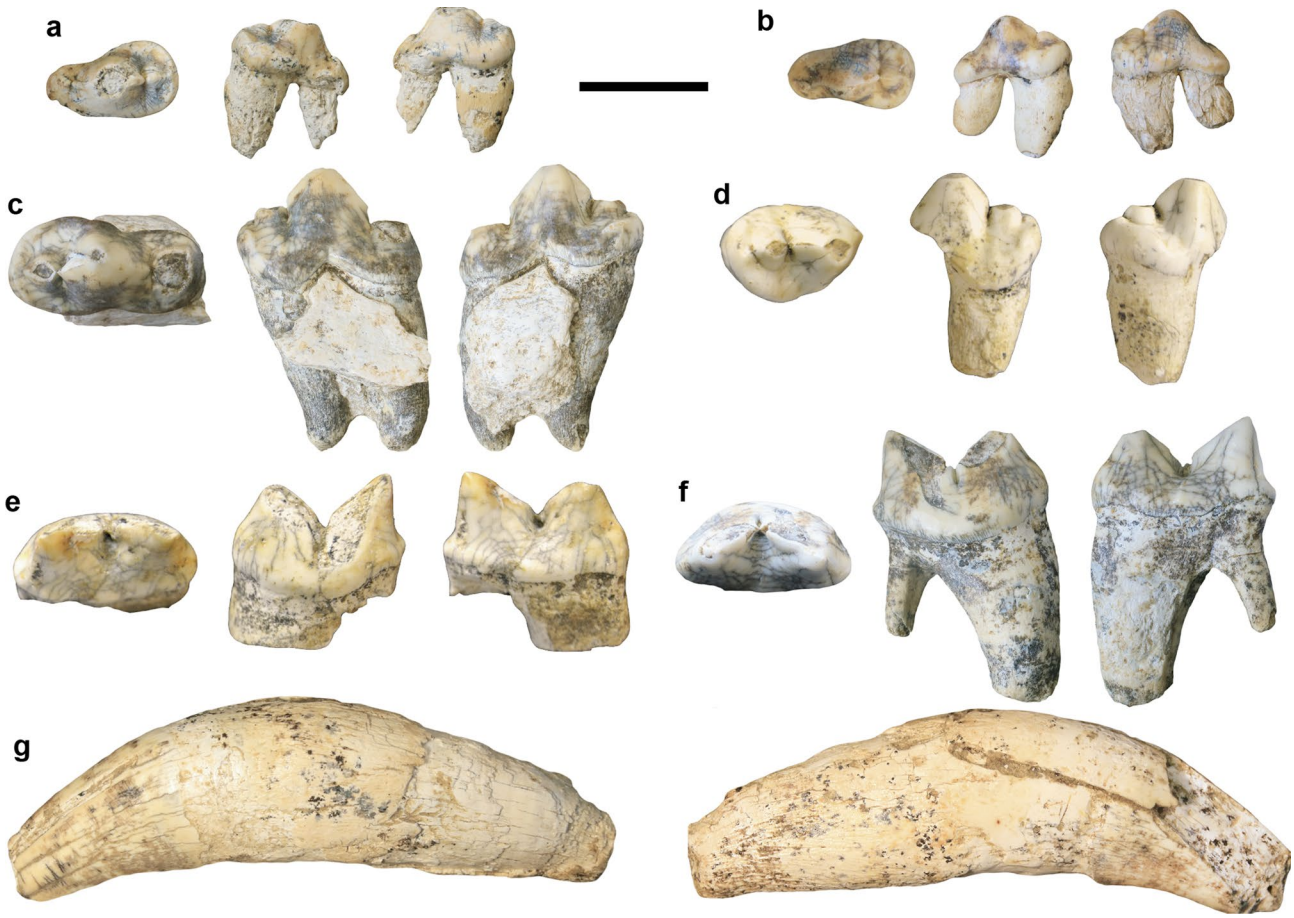

Fig. 5 Grotte de la Carrière lion dentognathic specimens from Sondage 1 in occlusal, buccal, and lingual views (from left to right). **a.** GDC2016-D5-29-Nv1, left p3. **b.** GDC2016-D67-255-Nv6, right p3. **c.** GDC2016-B4-Nv1, right p4. **d.** GDC2015-Pou-168, left distally fragmented p4. **e.** GDC2015-Pou-176, left m1. **f.** GDC2016-D6-64-Nv6, right m1. **g.** GDC2016-D6-37-Nv6, left c1 in buccal (left) and lingual (right) views. Scale bar equals 2 cm

Fig. 6 Grotte de la Carrière metacarpal bones from lower layers of Sondage 1 in proximal, dorsal, medial, ventral and lateral views (from left to right). **a.** GDC2016-D6-216-Nv6, right Mtc II. **b.** GDC2019-D5-545-Nv4, right Mtc II. **c.** GDC2015-D6-276-Nv8, left Mtc III. **d.** GDC2015-D7-21-Nv4, left Mtc III. **e.** GDC2016-D6-79-Nv6, left Mtc IV. **f.** GDC2019-C7-147-Nv4, right Mtc IV. Scale bar equals 2 cm

Description

Dental Remains Only one left c1 (GDC2016-D6-37-Nv6) was recovered. It belongs to an adult specimen. The tooth displays a moderate degree of wear. The apical part is partially fragmented, which prevent us from taking measurements (Fig. 5a). Nevertheless, two clear longitudinal ridges can be seen on the buccal side seen.

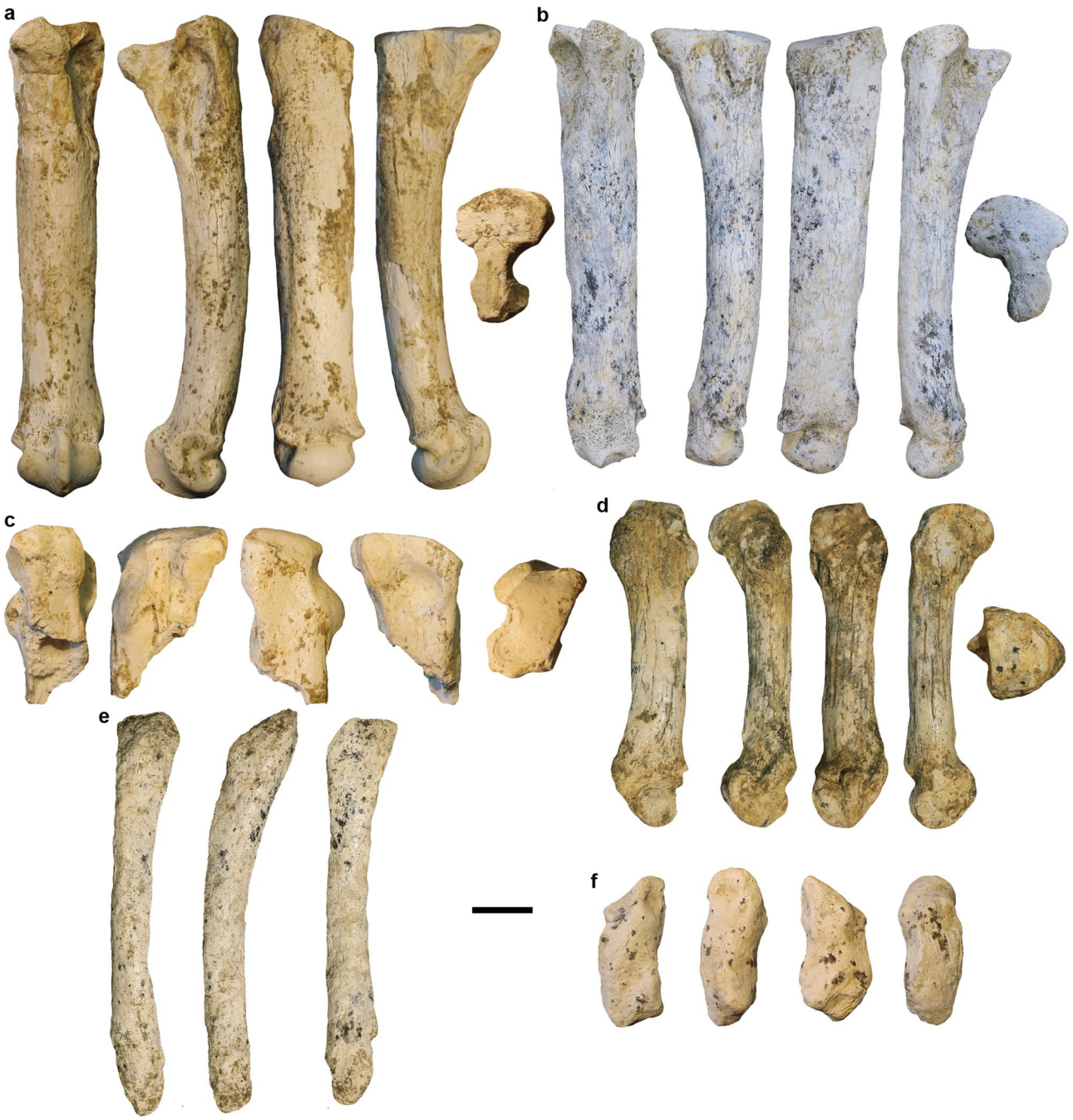

Fig. 7 Grotte de la Carrière metatarsal and metacarpal bones from lower layers of Sondage 1 in proximal, dorsal, medial, ventral, and lateral views. **a.** GDC2020-C5-11-Nv4, right Mtt III. **b.** GDC2016-D6-80-Nv4, left Mtt III. **c.** GDC2020-C5-314a-Nv4, proximal epiphysis of right Mtt IV. **d.** GDC2015-D6-283-Nv8, right MtcV. **e.** GDC2015-B6-98-Nv8, right Mtt V in dorsal, lateral and ventral view. **f.** GDC2020-D6-638-Nv4c, right MtcI in dorsal, medial, ventral and lateral view. Scale bar equals 2 cm

One left (GDC2016-D5-29-Nv1) and one right (GDC2016-D6-225-Nv6) p3 were studied (Fig. 5b–c). The shape of the buccal margin is slightly convex on its whole mesiodistal length. Both p3 protoconids are low and asymmetric in buccal view. Mesiolingually, a small and rounded paraconid is visible in occlusal view. Distally, a well-developed accessory cusp is characterized by a rounded morphology. Finally, a very incipient distal cingulum is visible, especially in GDC16-B5-29-Nv6 (Fig. 5b).

Regarding lower forth premolars, only right GDC16-B4-r-Nv6 (Fig. 5d) is complete. In the middle of the crown in buccal view, a high protoconid is well-separated from

Fig. 8 Grotte de la Carrière lion tarsal bones from Sondage 1. **a.** GDC2015-Pou-63, right astragalus in dorsal (left) and ventral (right) views. **b.** GDC2019-B7-579-Nv4, right astragalus in dorsal (left) and ventral (right) views. **c.** GDC2015-D6-318-Nv4, calcaneus in dorsal, medial, ventral and lateral views (from left to right). **d.** GDC2016-D6-122-Nv8, right astragalus in dorsal (upper) and ventral (down) views. **e.** GDC2020-C5-312-Nv4, right cuboid in proximal articulation facet (left) and distal articulation facet (right) views. **f.** GDC2020-C5-393-Nv4, left navicular in proximal articulation facet (left) and distal articulation facet (right) views. **g.** GDC2020-C5-313-Nv4, right navicular in proximal articulation facet (left) and distal articulation facet (right) views. **h.** GDC2020-C5-548-Nv4, cuneiform III in proximal articulation facet (left) and distal articulation facet (right) views

mesiobuccally placed paraconid and distal metaconid. Both are much smaller than the protoconid and relatively equally developed. A second tiny distal accessory cusp is visible attached to a distinct distal thin cingulum (Fig. 5d). The mesial margin is slender and uniform without any visible cingulum.

The two well-preserved isolated m1s were studied (Tables S6–S7; Fig. 5f–g). The protoconid is higher than the stouter paraconid, being comparable in mesiodistal length. Distally to the protoconid there is a small slightly developed talonid, both cusps are separated by a relatively deep notch. In occlusal view, this valley forms a V shape. In the middle of the lingual side, a tiny tubercle can be observed at the base of the crown. Distally, both m1s display a developed cingulum without any accessory cusp (Fig. 5f–g). In occlusal view, the crown is convexly curved. Its enamel presents a zigzag structure. Biometrically, p4 is practically equal in size to both studied m1s, being slightly larger (32.5 mm vs. 30.6 and 31.7 mm in GDC16-B4-r-Nv1, GDC15-Pou-176, and GDC16-D6-64-Nv6, respectively).

Axial Skeleton Two complete and well-preserved caudal vertebrae were recovered. The systematic description of caudal vertebrae (or the vertebral column in general) does not report any taxonomic information at the species level. However, the large size of both specimens suggests a large lion (Fig. S1b–c).

Appendicular Skeleton The lion forelimb skeleton specimens come from the lowest layers of Grotte de la Carrière and are represented by a right ulna and eleven metacarpals from at least two individuals: one Mtc I, three Mtc II, four Mtc III, two Mtc IV and one Mtc V (Table S5; Figs. 6 and 7).

Ulna The well-preserved fragment of a proximal right ulna includes the sigmoid cavity and the olecranon. The sigmoid cavity is concave and deep and forms a C shape in lateral view. An especially robust and elongated olecranon is proximal to the sigmoid cavity (75.4 mm and 30.4 mm anteroposterior and transverse diameter, respectively; Table 1), which displays clear scoring marks (Binford 1981) and pits (Online Resource 1, Fig. S1a). On the cranial surface of the proximal epiphysis is observed a significant depression for the triceps muscle insertion. The anterior part is broken. In general terms, GDC15-D6-37-Nv4 is anteroposteriorly stout.

Metacarpals A stout and short right Mtc I was recovered (GDC-D6-638-Nv4c; Fig. 7F). Two almost complete stoutly built right Mtc II (Fig. 6a–b) from distinct individual from that of the Mtc I (GDC-D6-638-4c) were preserved. The diaphysis of Mtc II is comparatively less straight and proximodistally large. The medial side of the proximal epiphysis is rectilinear. The shape of proximal epiphysis is triangular in proximal view, displaying an elliptical longitudinally developed facet on the lateral proximal side for Mtc III articulation. On the anterior side, a diagonal depression crosses the proximal epiphysis (strongly marked in GDC16-D6-216-Nv6; Fig. 6a).

Four Mtc III are preserved including two that are almost complete (right GDC-C6-17-Nv4 and left GDC-D7-21-Nv4; Fig. 6c–d) and one that is partially fragmented on the lateral side of proximal epiphysis (GDC-D6-276-Nv8; Fig. 6c). The two well-preserved proximal epiphyses (Fig. 6d) display a deep central depression in proximal view for the capitate carpal joint. The lateral articular facets for the Mtc IV articulation consist of one circular surface on the lateral anterior side and another one, elliptical and longitudinally expanded, on the lateral posterior side, similar to Mtc II. All the three metacarpals display a strongly marked depression on the anterior side of the proximal epiphysis. Contrary to Mtc II and Mtc III, the diaphyses of the two recovered Mtc IV are slender (Fig. 6e–f). The proximal epiphysis has a stout morphology. The single recovered Mtc V is well-preserved, the shaft is distally curved, and both epiphyses are stout (Fig. 7e). The medial side of the proximal epiphysis presents a large surface with a wide circular facet for the Mtc IV articulation (Fig. 6e).

Concerning the hindlimb skeleton, the bones recovered are represented by a fragmented fibula, one calcaneus (Fig. 8c), three right astragali (Fig. 8a, b, d), three cuneiform III (Fig. 8h), one cuboid (Fig. 8e), two naviculars (Fig. 8f–g), and five metatarsal bones: three Mtt III, one Mtt IV, and one Mtt V (Fig. 7).

Fibula The single right fibula (GDC2015-D6-182-Nv6) is partially fragmented on the proximal epiphysis. Only the distal epiphysis is relatively well-preserved. It shows an irregular rectangular shape with great relief in the distal tibiofibular joint, suggesting a powerful muscle insertion.

Calcaneus The posterior part of the calcaneus is fragmented (Fig. 8c). The calcaneal tubercle measures 87.63 mm in length, and on the superior surface, a strongly marked calcaneal tuberosity is present. On the inferior surface of this calcaneal tubercle, the sustentaculum tali emerges prominently from the anteromedial portion of calcaneus body. In general terms, the calcaneus is large and slender.

Astragalus All three preserved astragali display rounded borders in the neck and the body (Fig. 8a, b, d); the malleolar articulation, visible on the medial side of lateral trochlea, is partially fragmented (except in GDC-B7-579-Nv4), which prevents the measurement of maximal transverse diameter (Fig. 8). Between the lateral and the medial trochlear crests, there is an accentuated depth depression for the superior

tibia facet. The lateral trochlear crest is relatively distally oriented, towards the medial one, and is significantly larger. On the posterior part of astragalus body, the wide articular facets for the calcaneus insertion minimizes the calcaneal sulcus space. On the distal part, an especially stout neck and a large surface for the insertion of the navicular are visible (Fig. 8).

Cuneiform III Three cuneiforms III were recovered, all of them belonging to adults (Fig. 8h). GDC-C5-583-Nv4c is associated with a right third metatarsal GDC-S1-C5-11-Nv4, right cuboid GDC-C5-312-Nv4, and right navicular GDC-C5-313-Nv4.

Navicular Two almost complete oval naviculars were recovered from the same layer (L4) and square (C5) (Fig. 8f, g). Both conserve the wide surface for the astragalar insertion superiorly and for the cuneiform III posteriorly and are partially fragmented on the posterior side. Specimen GDC-C5-313-Nv4 belongs to the same individual as right Mtt III GDC-s1-C5-11-Nv4, right cuneiform III GDC-C5-583-Nv4c, and right cuboid GDC-C5-312-Nv4.

Cuboid GDC-C5-312-Nv4 is a well-preserved cuboid of an adult individual without any traces of damage (Fig. 8e). The tarsal bone articulates with Mtt IV GDC-C5-314-Nv4 and belongs to the same individual as right Mtt III GDC-C5-11-Nv4.

Metatarsal Three almost complete large and stoutly-built Mtt III were recovered (Fig. S7a, b). The asymmetrical "T" shape of the proximal epiphysis for the third cuneiform articulation is well-preserved in two of them (Fig. 7a, b). On the proximolateral side (Fig. 7a, b), the proximal epiphysis displays a deep fossa for the Mtt IV articulation. The fragmented right Mtt IV GDC-s1-C5-314-Nv4 (Fig. 7d) preserves only the proximal epiphysis. In proximal view, the proximal epiphyseal surface for the cuboid bone insertion is asymmetrically quadrangular (Fig. 7c). This Mtt IV is associated with Mtt III GDC-C5-11-Nv4 and cuboid GDC-C5-312-Nv4. Finally, the only recovered Mtt V (Fig. 7d) is distally fragmented and presents strong traces of weathering and corrosion on the bone surface along the diaphysis, precluding accurate morphological description (This issue is present in all the bones recovered but is especially prominent in Mtt V).

Phalanges Twenty-five phalanges from the anterior and posterior paws were recovered, thirteen Ph I (Fig. S2) and twelve Ph II (Fig. S2). All of them are almost complete and belong to adult or subadult individuals. The right Ph I GDC-C5-394a-Nv4 (Fig. S2i) and Ph II GDC-s1-C5-314b-Nv4 (Fig. S3d) associate with the right Mtt III GDC-s1-C5-11-Nv4 (Fig. 7b).

For further information on the studied specimens unearthed from the Middle Pleistocene layers of Grotte de la Carrière, the reader is referred to Online Resource 1.

Results

Morphological Comparisons with Middle and Late Pleistocene Lions

The European Pleistocene lions are similar to one another both morphologically and metrically (Argant et al. 2007). Notwithstanding, the large size of Middle Pleistocene lions has been noted by numerous authors (Schütt 1969; Schütt and Hemmer 1978; Argant 1988, 1991; Argant et al. 2007; Marciszak et al. 2019, 2021). Historically, the phylogenetic position and taxonomy of fossil lion species was mainly based on dentognathic morphology (Schütt 1969; Schütt and Hemmer 1978; Argant 1988, 1991; Sotnikova and Nikolskiy 2006; Hankó, 2007; Marciszak and Stefaniak 2010, Sabol 2014). Accordingly, the premolars of *P. fossilis* differ from those of *P. spelaea* in the following aspects: more robust p3 crown (Marciszak et al. 2021); slightly convex buccal margin on the whole p3 (Marciszak and Stefaniak 2010); elongated and high protoconid in p3 (Marciszak et al. 2021); presence of well-developed anterior and posterior cusps, namely paraconid and hypoconid (= metaconid; Baycka 2008), respectively, in p4 (Schütt and Hemmer 1978; Ballesio 1980; Hankó 2007; Barycka 2008); shorter and higher protoconid in p4 (Schütt and Hemmer 1978); premolars, especially p4, proportionally larger than m1 (Schütt and Hemmer 1978; Argant 1988, 1991; Barycka 2008); elongated p4 with respect to total length of m1 within the same mandibular fragment (Schütt 1969; Schütt and Hemmer 1978; Sabol 2014; Marciszak et al. 2017; Fig. 5). *P. fossilis* is also distinguishable from *P. spelaea* in the following m1 characters: wider m1 crown (Schütt and Hemmer 1978; Ballesio 1980); higher and sharper protoconid and rounded robust lower portion of the paraconid (Thenius 1972); mesially oriented protoconid edge (Fig. 5; Hankó, 2007); more developed posterior talonid in m1 (Schütt 1969; Schütt and Hemmer 1978; Argant et al. 2007; Hankó 2007; Argant and Brugal 2017); presence of mediolingual protuberance or bulge at the base of the crown (Schütt 1969; Schütt and Hemmer 1978; Hankó 2007; Argant and Brugal 2017; Marciszak et al. 2021); presence of zig-zag enamel structures (Schütt and Hemmer 1978; Barycka 2008); and well-developed abrupt curve of the enamel, on the buccal side, in occlusal direction, that rises below the protoconid and produces a convex shape margin of the whole m1 (Hankó 2007). Lastly, as a consequence of a wider m1 crown, the teeth have a higher B/T ratio (Schütt 1969; Hemmer and Schütt, 1970; Schütt and

Hemmer 1978; Ballesio, 1980); according to Marciszak and Stefaniak (2010), this ratio has an average value of 0.54 for *P. fossilis* (range from 0.47–0.58) and 0.5 for *P. spelaea* (range from 0.36–0.57).

Despite the high reliability of teeth for taxonomic purposes, the postcranial skeleton may help when the dentognathic remains are scarce (Barycka 2008; Sotnikova and Foronova 2014; Marciszak et al. 2019). The interspecific differences of limb bones have been observed both dimensionally and proportionally. According to Argant and Brugal (2017) and Marciszak et al. (2019, 2021), the chronologically older *P. fossilis* showed an increase in size until MIS11-9, when the largest individuals are recorded. From this moment on, size in fossil lions decreased until they reached a size similar to that of extant African lions. The main problem in considering this simplified size-reduction trend is that it does not seem to respond only to chronological proxies. Indeed, it is necessary to consider the different biotope inhabited, which depends on the climate, the faunal communities, and intraspecific differences, especially sexual dimorphism (see Table S8 for our analysis on the sexual dimorphism of extant lions).

Focusing our attention in the morphological characters, the specimens described in this study share the diagnostic features reported for *P. fossilis,* namely (Schütt 1969; Schütt and Hemmer 1978; Argant 1988, 1991; Argant et al. 2007; Hankó 2007; Barycka 2008; Marciszak and Stefaniak 2010; Marciszak et al. 2019, 2021): markedly wide m1 at the base of the crown, larger premolars (Tables S9 and S10), high and sharp protoconid edge and short rounded paraconid edge in m1, mesially oriented edge of the protoconid of m1, small lingual protuberance in the medial part of m1 crown, the zig-zag structure in the m1 crown's enamel - taxonomically used by some authors who considered that a common character related to Middle Pleistocene lions (Marciszak and Stefaniak 2010) but questioned by others (Sabol 2014), proportionally short paraconid and oval and slightly convex buccal margin in both p3, presence of abrupt curve in the buccal enamel in m1 that rises below the protoconid, B/T ratio close to *P. fossilis* average (Table S1), stoutly-built astragalus (Fig. 8), large calcaneus, anteroposteriorly stout ulna, robust proximal and distal epiphyses of third and fourth metacarpals and third metatarsal (Figs. 6 and 7). On the other hand, the analyzed specimens differ from previously reported *P. fossilis* in: the slightly developed posterior talonid in m1, absence of the groove at the top of the medial lingual protuberance of the m1 (Schütt 1969; Schütt and Hemmer 1978; Argant and Brugal 2017), slender calcaneum, and proportionally proximodistally short metatarsus and metacarpus.

In summary, based on morphological characteristics described and compared above, the specimens from Grotte de la Carrière can be referred here to *Panthera fossilis*. The combination of morphological similarities with *P. spelaea* in the dental remains and of the tendency of postcranial remains such as tarsal and metapodial bones to be stouter, as in *P. fossilis*, further suggest the presence of intermediate features towards late Pleistocene European lions.

Biometrical Comparisons with European Pleistocene Lions

The morphometric differences between European lion groups over geological time normally follow the diagnostic features related to dentognathic remains (Schütt 1969; Argant 1991, 2010; Hankó 2007; Sabol, 2014). Alternatively, several researchers have also included the proportions of postcranial in statistical analyses (Dietrich 1968; Ballesio 1980; Bona and Sardella 2012; Baryshnikov 2016; Sotnikova and Foronova 2014; Marciszak et al. 2019). In the present study, biometrical comparisons are focused on lower dental remains and several morphometric characters of postcranial bones, such as tarsals and metapodials. To maximize intergroup differences and to avoid intraspecific variation, we chose those variables with significant intergroup differences supported by statistical tests have been observed: one-way ANOVA ($p < 0.05$) for parametric variables and Mann–Whitney pairwise ($p < 0.05$) for non-parametric. The complete measurements are shown in Table 1 and the statistically significant comparisons in Table S11.

Dental Remains

In general terms, European lions display a trend of decreasing size over time from the Middle Pleistocene forms to their most recent relatives (Marciszak and Stefaniak 2010; Marciszak et al. 2019). Nevertheless, the decrease of middle Middle Pleistocene lions to the two younger groups of Late Pleistocene and the extant African lions is not always observed in the geologically older group from MIS 15–12. These forms usually show smaller values compared with those from MIS 11–9 (Marciszak et al. 2019). Notwithstanding, the extant relatives and the MIS 5e-2 lions were significantly smaller than the massive, large lions from the early and middle Middle Pleistocene (Fig. 9a).

The above-mentioned chronological decreasing trend of size was firstly observed in the lower dental remains (Fig. 9a). In the lower m1 B/TL ratio (Fig. 9a), this trend is easily followed from MIS 15 to latest Pleistocene ones, with the GDC specimens better grouped with MIS 11–9 forms, as expected. The box plots depicted from the premolars (Fig. 9a) show that the smaller specimens are the ones of the MIS 15–12 group. Moreover, MIS 5e-2 is larger than MIS 8–6 in the p4 B/TL (Fig. 9a). GDC values fit in the middle Middle Pleistocene box, much closer to the median point of MIS 11–9 box (Fig. 9a).

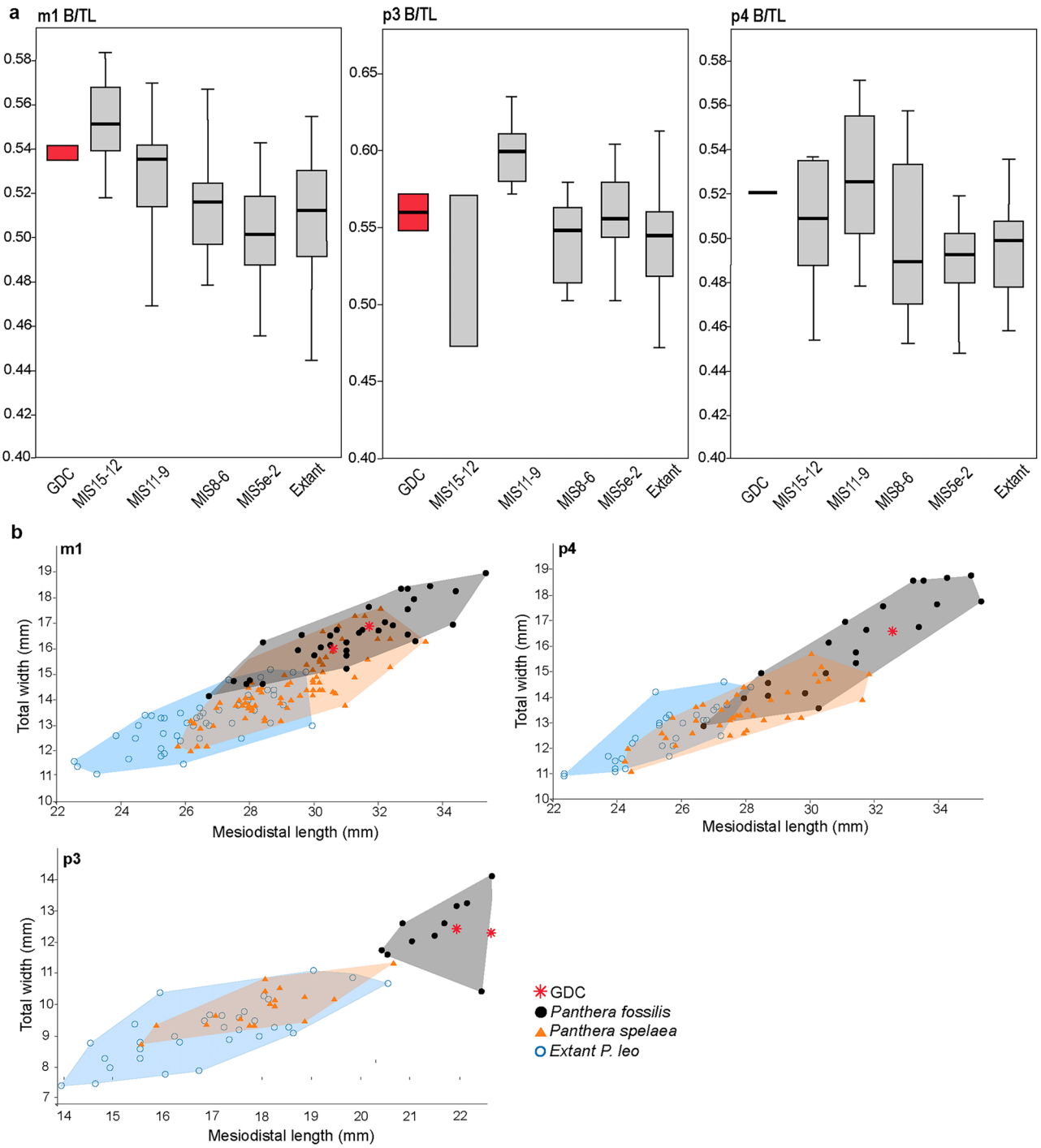

Fig. 9 **a.** Boxplots of total breadth to total length B/TL ratio of lower dental remains from Grotte de la Carrière, Middle to Late Pleistocene localities and extant relatives showing the chronological trend. **b.** bivariate graphs of total width against total length of lower dental remains

Concerning interspecific differences, the studied specimens were compared to both European lions, *P. fossilis* and *P. spelaea,* as well as extant *P. leo*. We included the *P. intermedia* m1 values from Igue de Rameaux in the *P. spelaea* group, as they are biometrically indistinguishable. Complete measurements of Grotte de la Carrière specimens can be found in Table 1. In Fig. 9b are represented the scatter plot diagrams for maximum breadth against total length for m1, p4, and p3. The one-way ANOVA corroborates the statistical significance of results (see Table S11).

In the scatter diagrams for p3 and p4 are observed some clear intergroup differences (Fig. 9b). The set of *P. fossilis* p3 variables are in the uppermost part of the plot, separated from *P. spelaea* and *P. leo* values (Fig. 9b). Concerning the p4 bivariate graph, *P. fossilis* values are located in the uppermost part (Fig. 9b). In this case, overlapping groups of species can be observed in the lowermost part of the convex hull. In both premolars, the GDC specimens overlap the uppermost part of *P. fossilis* variance (Fig. 9b). As regards the m1 (Fig. 9b), GDC m1 fits within the *P. fossilis* cloud, near the uppermost *P. spelaea* area (population from Lherm and Azé I-3), in the fringe between both species. In detail, GDC values are located closest to *P. fossilis* from Westbury, Petralona, Aragó, and Vértesszölös II and *P. spelaea* from Lherm and Azé I-3.

According to some authors (Schütt 1969; Hemmer and Schütt, 1970; Schütt and Hemmer 1978; Ballesio 1980), the m1 B/TL coefficient can be used to separate *P. fossilis* from *P. spelaea.* In the former, this ratio is normally above 0.47–0.58, whereas in the latter, the ratio normally is 0.36–0.57 (Marciszak and Stefaniak 2010). The GDC sample matches better with *P. fossilis* (0.54) (Table S6).

Tarsal Bones

Among the postcranial elements, the tarsal and metapodial bones have significant results for interspecific correlations (Sabol 2014). In tarsal bones, the chronological trend of decreasing size over time seen in dental remains is also normally displayed (Fig. 10a). However, lions from MIS 5e-2 experienced an increase in size compared to the chronologically older MIS 8–6 group, a tendency also observed between MIS 11–9 and MIS 15–12 for the calcaneus values (Fig. 10a). The tarsal bones were compared to both classical Pleistocene European lions: *P. spelaea* and *P. fossilis*. Complete measurements are in Table 1. In Fig. 10b are represented the bivariate graphs for astragalus/calcaneus, plotting the maximum mediolateral diameter against total proximodistal length, with the graphical representation of MD/L and TL ratio in boxplots.

Astragalus The statistically significant results for the maximum mediolateral diameter to the total length ratio MD/TL for the astragalus point out a clear division between the two species and reflect how Late Pleistocene *P. spelaea* differs from the Middle Pleistocene ones based on smaller size (Fig. 10a). Contrary to the observed analysis for the dental remains, the set of variables from MIS 11–9 shows a decreasing size tendency with respect to the older MIS 15–12. The MIS 8–6 group instead, has significantly reduced size compared to the most recent group, MIS5e-2. GDC values are located at the top level of the MIS 11–9 box and at the uppermost MIS 5e-2. In the resulting bivariate graph, the values are perfectly separated into two clouds of points (Fig. 10b). In the uppermost part of the graph, where GDC specimens fit, are located the *P. fossilis* individuals. GDC-s1-Pou-63, in which the partially rounded bone affected the measurement of maximum transversal diameter, is located outside the *P. fossilis* range, near one specimen from Zá Hájovnou Cave.

Calcaneus In the MD/TL ratio for calcaneus, the trend is not as clear as the one for the astragalus (Fig. 10a). The differences are also not statistically significant. Nevertheless, the *P. fossilis* groups from middle Middle Pleistocene differ statistically in the total length of calcaneus from *P. spelaea* and *P. intermedia* from MIS 8–6 and MIS 5e-2 (Fig. 10a). In the bivariate graph, the uppermost part corresponds to *P. fossilis* values and the lowermost part to *P. spelaea* (Fig. 10b). The single GDC specimen fits within the *P. fossilis* variability, near the edge of the *P. spelaea* cloud where the highest values are located, for Lezetxiki VI and within the Château range.

Metapodial Bones

The taxonomic reliability of the metacarpus and metatarsus is rather poor. These features present an intraspecific variation related generally to the locomotor apparatus in relationship with the habitat (Turner 2009). In general, autopodial bones are practically indistinguishable from one to another. In the comparison below, we included European and North American fossil lions from MIS 15–2 to recent lions and focused only on variables in which the intergroup differences were supported by statistical tests (Mann–Whitney test, $p > 0.05$; Tables S1, S2, S7 and S11). In Figs. 11 and 12 are represented in boxplots the significant interspecific indices.

In general terms, the *P. spelaea* from MIS 5e-2 and the extant lions are less stoutly-built than the ancient *P. fossilis* and North American *P. atrox*. The recent lions differ from the rest of the groups in the slenderness of both epiphysis and the shorter diaphysis. In *P. fossilis* from Poland MIS 9–10 and *P. spelaea* from MIS 6 of Lherm (France), relatively larger values have been noticed in comparison to others of their own groups in the maximum anteroposterior diameter of the proximal epiphysis and the proximodistaly larger diaphysis.

The intergroup differences that are statistically significant for the Mtc III include total length and maximum anteroposterior diameter of proximal and distal epiphysis (Fig. 11). For Mtc IV, they are total length, maximum anteroposterior diameter of proximal epiphysis, maximum transverse middle shaft diameter and maximum transversal diameter of distal epiphysis (Fig. 11). For Mtt III, they are: total length, maximum anteroposterior and transversal diameter of proximal epiphysis,

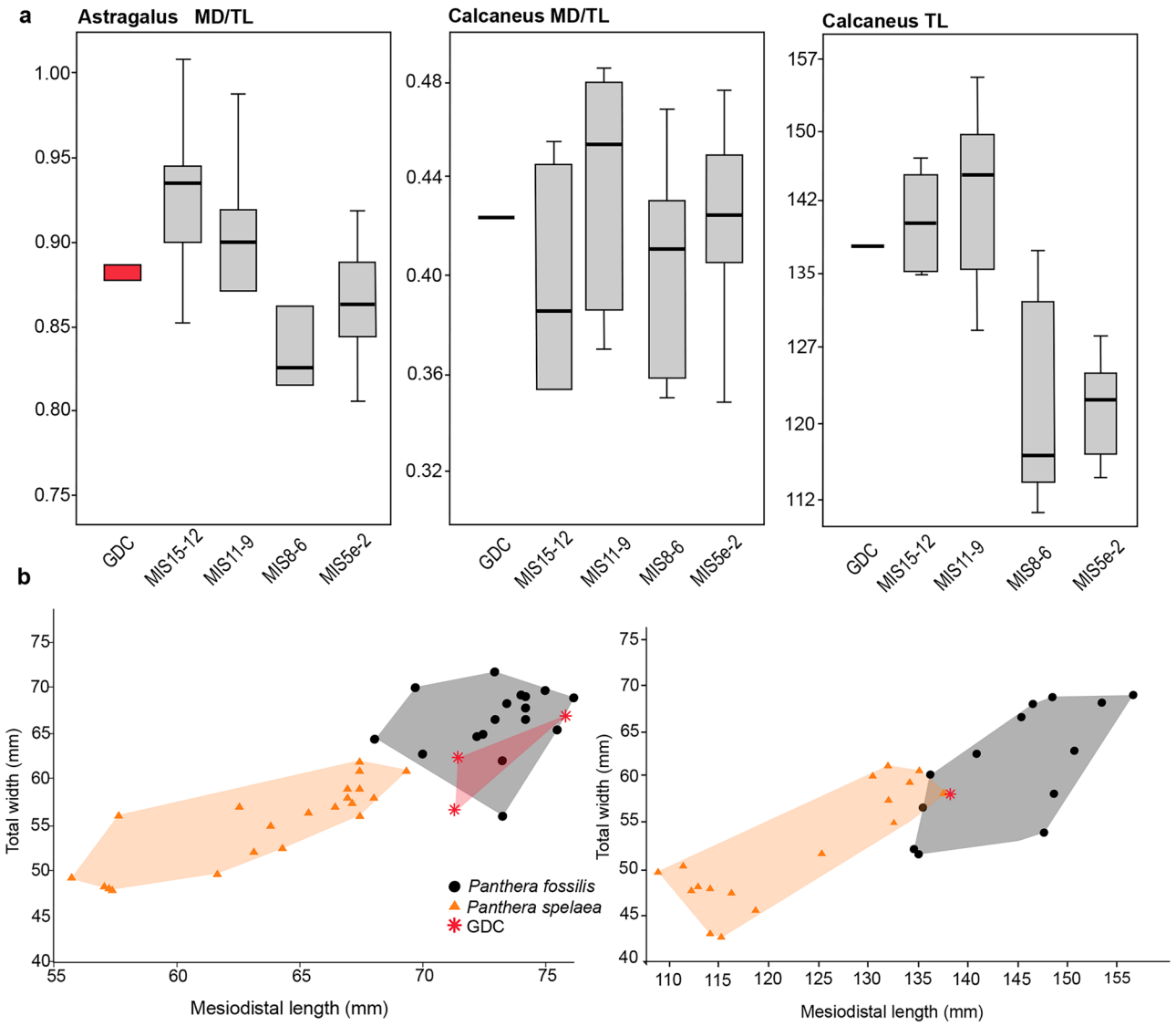

Fig. 10 **a.** Boxplots of select ratios of tarsal bones from Grotte de la Carrière, Middle to Late Pleistocene localities showing the chronological trend. **b.** bivariate graphs of total width against total length of astragalus (left) and calcaneus (right)

and maximum transversal diameter of distal epiphysis (Fig. 12). Checking the resulting boxplots for the ratio between Dpap/TL and Ddap/TL of Mtc III and Mtc IV (Fig. 11), the midpoint of the GDC data is closer to the top or midpoint of the *P. fossilis* box, except Ddap/TL of Mtc IV, which are near the bottom (Fig. 11).

According to the performed analyses, the GDC specimens are significantly distinct from *P. spelaea* in maximum anteroposterior diameter of the proximal epiphysis of metacarpals III and IV (Fig. 11) and maximum anteroposterior and mediolateral diameter of the proximal epiphysis of metatarsal III (Fig. 12). None of the metacarpals nor metatarsals from GDC shows a statistically significant distinction compared with *P. fossilis*.

In summary, the trend observed shows that middle Middle Pleistocene *P. fossilis* are significantly distinguishable in proportions from Late Pleistocene European and North American lions and their extant African relatives. Generally, the studied specimens differ from Middle Pleistocene lions *P. fossilis* in total length but are similar to them in anteroposterior and mediolateral diameter of the proximal epiphyses, a feature especially prominent in Mtt III (Fig. 12).

Discussion

Grotte de la Carrière Lions in the Context of Middle Pleistocene European Lions

As discussed in the biometrical comparisons section, the fossil remains of *P. fossilis* from Grotte de la Carrière reveal stout

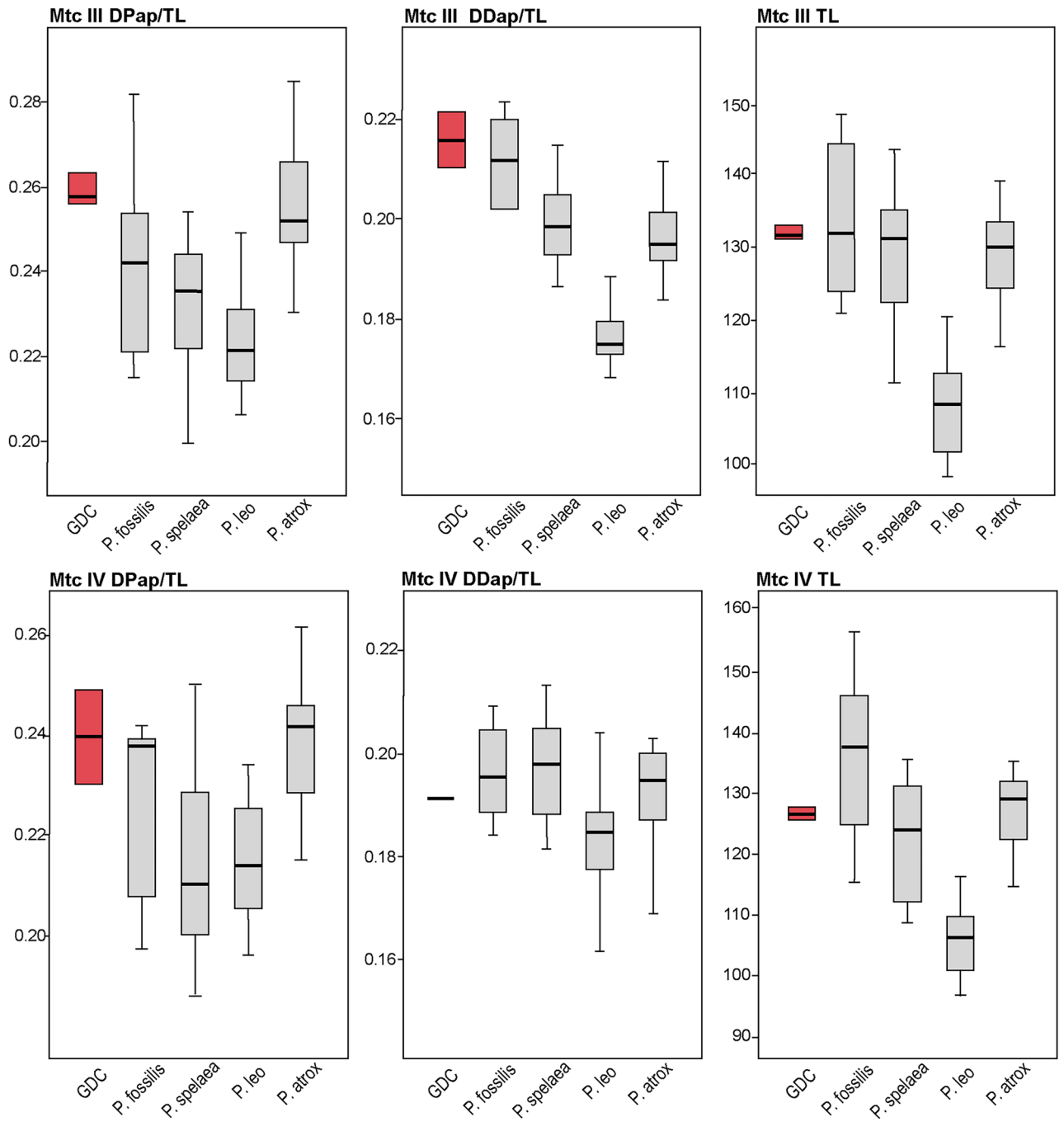

Fig. 11 Boxplots of select ratios and measurements of Grotte de la Carrière metacarpal bones (marked in red) compared to *Panthera fossilis*, *Panthera spelaea*, *Panthera atrox* and values for extant relatives

and relatively large specimens, fitting within the size range and morphology of this species from coeval sites (middle Middle Pleistocene, MIS 11–9). The specimens from Sima de los Huesos from the Atapuerca complex (Iberian Peninsula), Vértesszölös 2 (Hungary), and Zá Hájovnou from Moravia (Czech Republic) are the similar to Grotte de la Carrière individuals and also proportionally larger than Petralona (Greece), Torre in Pietra (Italian Peninsula), Kent's Cavern (Great Britain), and Lunel-Viel and Orgnac (France) samples. In contrast, those individuals from the Polish localities of Biśnik and Wierzchowska, predominantly from steppe-tundra and boreal forest landscape, are especially large. The harsh and cold ecosystems in which they lived could explain their larger size following Bergmann's Rule (Bergmann 1847).

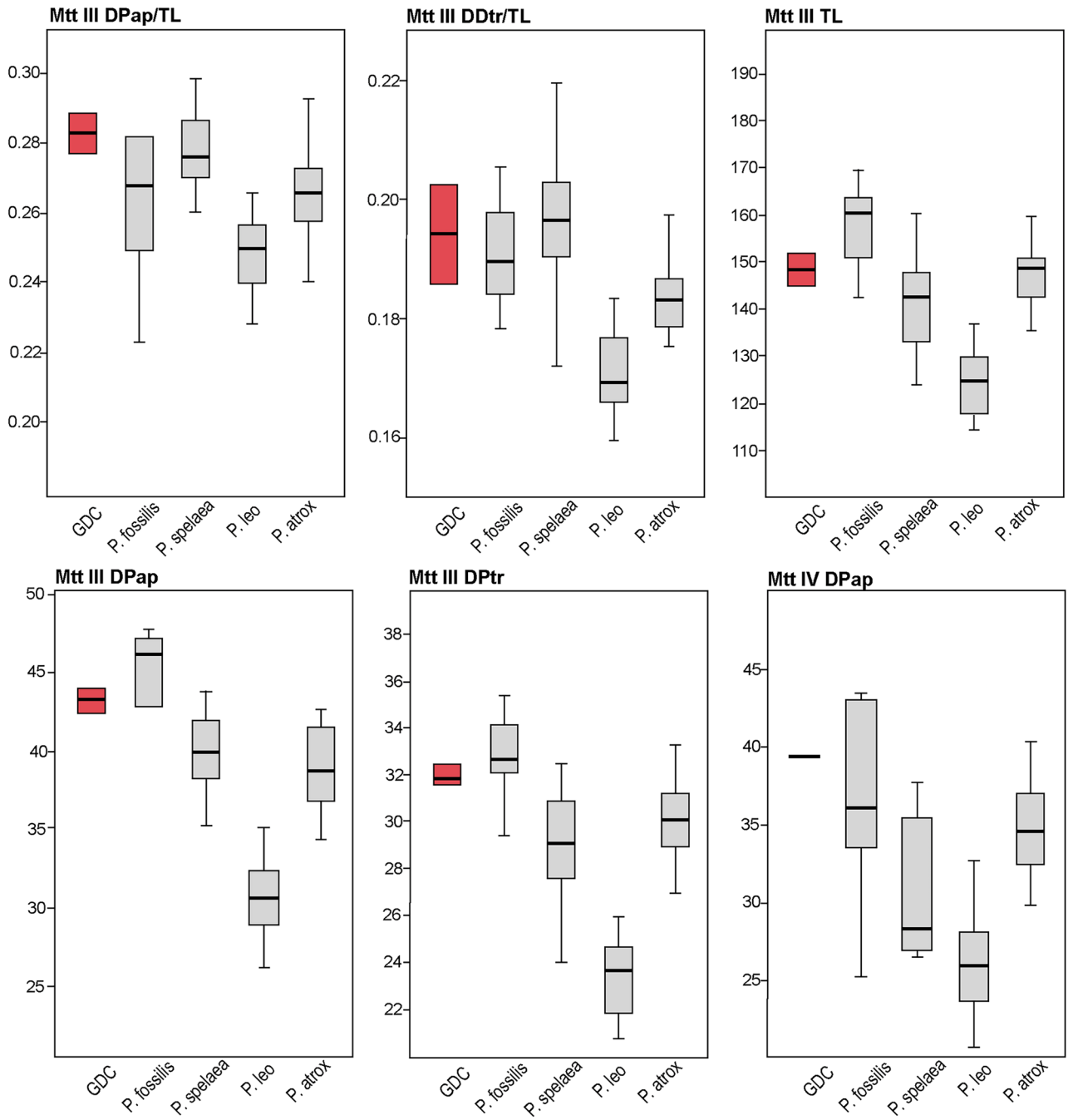

Fig. 12 Boxplots of select ratios and measurements of Grotte de la Carrière metatarsal bones (marked in red) compared to *Panthera fossilis*, *Panthera spelaea*, *Panthera atrox* and values for extant relatives

Bergman's Rule proposes a heat balance explanation for the differences in body size depending on the latitudinal distribution of species (Bergmann 1847). In general, the gradient of body size increase with the latitude (in accordance with increasingly cold conditions). Not all species fit Bergman's Rule because there are other factors to take into consideration. In this case, the differences in the biomes such as the Mediterranean vegetation (e.g., Torre in Pietra, Sima de los Huesos, and Petralona) and steppe/tundra (Biśnik and Wierzchowska) or alpine boreal forest (Zá Hájovnou) may affect the biocenosis.

Traditionally in the paleontological literature, the steppe lion has been considered a predator adapted to wide variety of ecosystems (Hemmer 2004; Turner 2009). Bearing in mind that each biotic community is naturally adjusted according to its local climate and that the locomotor apparatus is

linked to predatory strategies (Moore and Biewener 2015), species adaptations to distinct biomes may reflect regional differences in the skeleton. For example, European terrestrial biomes usually encompassed grassland, forest, and tundra. Consequently, the prey spectrum available and hunting strategies are distinct for each one. In particular, for ambushing prey hunters wait for the prey and launch one quick strike (Moore and Biewener 2015), so this type of predatory behavior strategy has specific skeletal requirements. To illustrate, recent studies report that extant male lions use the savanna vegetation for ambushing prey instead of pursuit in open grasslands like female lions (Loarie et al. 2013).

According to the last assertions, the inhabitants of steppe-tundra would prey on woolly mammoth (*Mammuthus primigenius*) and rhinoceros (*Coelodonta antiquitatis*), giant deer (*Megaloceros giganteus*) or elks (*Alces alces*) beyond the northern boundary of boreal or deciduous forest (Kahlke 2014). Those lions from Western Europe, which inhabited deciduous/mixed or mountainous forests with steep cliffs, far from the ice sheet cover during glacial periods (Fig. 1), probably preyed on large red deer (*Cervus elaphus),* the fallow deer (*Dama dama*), the steppe bison (*Bison priscus*), the rhinoceros (*Stephanorhinus hemitoechus*), and cave bear (*Ursus deningeri* or *U. spelaeus* s.l.) and occasionally on relatively smaller roe deer (*Capreolus capreolus*), ibex (*Capra Ibex*), and chamois (*Rupicapra rupicapra*).

Regarding the case of Biśnik Cave, the fossil remains were deposited on the cavity during the Odra Glaciation, when the typical steppe tundra dominated these habitats, a landscape dominated by wooly rhinoceros (*Coelodonta antiquitatis*) and steppe bison (*Bison priscus*). These conditions favored long proportions, especially in the metapodials, whereas the proportions of Grotte de la Carrière lions resemble those from the inhabitants of forest biomes. The presence of species well adapted to rocky environments such as the genus *Hemitragus* or the roe deer (*Capreolus capreolus*) (Demay et el. 2020 and references therein) suggest a mountainous forest, probably with steep cliffs. The mammal assemblage from MIS 9 layers of Caune de l' Arago (50 km northeast of Grotte de la Carrière), formed by *Cervus elaphus, Bison priscus*, *Equus ferus,* and *Stephanorhinus* (Moigne et al. 2006), spans a wider spectrum of species adapted to more open grasslands, the same conditions as in Moravian localities. To sum up, the lions from the above-mentioned Polish localities and surrounding areas probably tended to be stouter and larger, conditioned by the surrounding biome.

Comparisons with the Earliest Lions from Middle Middle Pleistocene MIS 15–12

Following the size trend observed by Marciszak et al. (2019), the studied material from Grotte de la Carrière should be in general larger than major part of chronologically older lions from MIS 15–12. This implicit trend is fulfilled by most fossiliferous sites, except the northeastern France locality of Breccia de Château and the Central European sites of Moggaster and Poludniowa, in which they are larger and stouter. The studied specimens from Westbury and Caune de l' Arago share similar characteristics with GDC lions.

The intraspecific distinctions between the larger specimens from Central Europe could be a response to climatic dynamics and geographical settings, as has been seen with the coeval sites. Traditionally, climatic events strongly influenced the biogeographical distributions of mammalian species and influenced the faunal associations of regional biomes (Rodríguez et al. 2004). The earliest glaciation period (MIS 16–13) from the Middle Pleistocene occurred at the same time for all European regions (Head and Gibbard 2005). It is characterized by non-glacial cooling during cold stages (Candy et al. 2010, 2014; Lindner et al. 2013), succeeded by less interglacial warming compared to MIS 11–9 (Szymanek and Julien 2018). The Mid-Brunhes Transition (ca. 430 ka) marks the increase in the amplitude of the climate cycles to 100 kyr (Jansen et al. 1986; Elderfield et al. 2012). So, the strong glacial dynamics and the development of regular icesheet covering during cold stages started in MIS 12–10 (Böse et al. 2012) with the arrival of the so-called Elster glaciation across northern Europe (Kahlke et al. 2011; Ehlers et al. 2011), also known as Mindel in the Alpine region and Anglian in Great Britain. Consequently, the increase in body size may be related to these climatic fluctuations, as an adaptation to the resulting new cold conditions and the latitudinal changes in the biomes (Rodríguez et al. 2004). Indeed, that could explain the coincidence among the large and stout lions' occurrence with the strong climatic events of MIS 12–10.

In Central and Northern Europe, the cold-adapted large mammals of the *Mammuthus-Coelodonta* steppe complex were established then for the first time (Kahlke et al. 2011; Szymanek and Julien 2018). Some studies have revealed that the increase in body size may be related to the expansion of this so-called '*Mammuthus-Coelodonta* steppe' as an adaptation to the resulting new biome. The mammal assemblage of Mosbach and other localities from the Great European Plains suggest a sequence of changes in ecological conditions usually dominated by dry steppe-tundra landscapes occasionally interrupted by the extension of deciduous and mixed forest during warmer and wet climatic episodes (Kahlke et al. 2011). Instead, in southwestern Mediterranean regions, including southern France and the Great Britain site of Westbury, the climate during MIS 13–7 intervals was generally temperate (Szymanek and Julien, 2018; López-García et al. 2021), less cold than in Central Europe. That favored the expansion of deciduous

areas. Precisely, the largest individuals from Moggaster and Poludniowa come from the steppe-tundra, areas in which extreme climatic conditions, prey availability (and thus the hunting strategies), and interspecific competition forced individuals to be stouter.

Unfortunately, all the factors that affect the body size structure of large mammals are difficult to analyze due to the lack of available specimens in the known fossiliferous sites.

Comparisons with Transitional Forms from Late Middle Pleistocene MIS 8–6

According to Marciszak and Stefaniak (2010), the forms between MIS 9–6 normally possesses intermediate characteristics, especially those around MIS 7-5e. The specimens from GDC presents some intermediate features, especially in the biometric dimensions the of metapodial bones and the proportions of m1, which resemble the ones of *P. spelaea.* Argant and Brugal (2017) describe the lion from Igue-de-Rameaux as a distinct species with intermediate features, namely *Panthera intermedia*, and include in its hypodigm individuals from the French localities of Abimes de la Fage (MIS 7, France), Romain la Roche (MIS 6), and Orgnac III (MIS 9). Compared to them, the Grotte de la Carrière sample has some morphometrical resemblances including the reduced talonid and the absence of a tiny groove at the top of the medial lingual protuberance of m1 and the proximo-distally shorter metacarpals and metatarsals in the case of Romain la-Roche and Orgnac III specimens. However, the size of dental remains is proportionally larger than in the Abimes de la Fage and Romain la Roche samples and similar to large-sized specimens from Igue de Rameaux. The lion remains from the rest of the fossiliferous sites of Central-Eastern Europe MIS 8–6 are attributed to *P. fossilis*, whereas in the western France localities of Lherm, Santenay, and Azé I-3, the lions are referred to the *P. spelaea* group. This complexity in the characters of populations, considering the chronology of the studied sites, is expected. Notwithstanding, the lions from Lherm differ substantially from the rest by their larger dimensions, similar to the *P. fossilis* of the Middle Pleistocene, almost equal to Grotte de la Carrière lions. As seen above, geography is not the only factor that influences species variability. Considering the chronology of Lherm, those lions lived in glacial conditions. In this case, Bergman's rule should not be ruled out, for which the mammals in cold regions have the trend to be stouter and larger than the individuals of the same species living in warmer sites. Finally, it should not be forgotten that due to European regional differences, the replacement *P. fossilis-P. spelaea* probably occurred at different times (Marciszak et al. 2014).

Conclusions

On the basis of the morphological and morphometric analysis performed in the present study, the Grotte de la Carrière large felid remains are included in the hypodigm of the species *Panthera fossilis* (von Reichenau, 1906). The studied lion from the Réseau Lachambre karstic complex, with an estimated chronology corresponding to the MIS 9 interglacial, shares several dental diagnostic features and body proportions related to previously recorded Middle Pleistocene forms from the interval MIS 11–9. Nevertheless, some minor features more closely resemble later *P. spelaea* European forms from MIS 8–6. Such later forms have also been called 'intermediate forms' by previous authors, between the two species of the European lion lineage. The reported data can shed new light on the still scarcely recorded Northern Hemisphere lions and their size trends over the Pleistocene putatively related to climatic shifts and environmental parameters.

Supplementary Information The online version contains supplementary material available at https://doi.org/10.1007/s10914-022-09600-0.

Acknowledgements The authors want to express their gratitude to Philippe Galant, Jean Louis-Perez, Michel Gomez and Jêrome Durbet for their help and availability during the field work at the Têt Valley and to Darin Croft, the associate editors and two anonymous reviewers for improve an early version of this manuscript.

Authors Contributions All authors contributed to the study conception and design. Material preparation, data collection and analysis were performed by Maria Prat-Vericat, Adrian Marciszak and Joan Madurell-Malapeira. The first draft of the manuscript was written by Maria Prat-Vericat and all authors commented on previous versions of the manuscript. All authors read and approved the final manuscript.

Funding Open Access Funding provided by Universitat Autonoma de Barcelona. This work has been funded by the Direction Regionalle des Affaires Culturelles of the French Government (DRAC Occitaine) and the Agencia Estatal de Investigación-European Regional Development Fund of the European Union (CGL2017-82654-P, AEI/FEDER-UE) and the Generalitat de Catalunya (CERCA Program). J.M.-M. is member of the consolidated research group 2017 SGR 116 (AGAUR, Generalitat de Catalunya). LS is supported by the FI AGAUR fellowship (ref. 2020 FI_B1 00131) funded by the Secretaria d'Universitats i Recerca de la Generalitat de Catalunya and the European Social Fund.

Availability of Data and Material The datasets generated during and/or analyzed during the current study are available in the Online Resource 1.

References

Altuna J (1972). Fauna de mamíferos de los yacimientos prehistóricos de Guipúzcoa, con catálogo de los mamíferos cuaternarios del Cantábrico y del Pirineo occidental. Munibe 24:1–464.

Álvarez-Lao DJ, Álvarez-Vena A, Ballesteros D, García N, Laplana C (2020) A cave lion (*Panthera spelaea*) skeleton from Torca del León (NW Iberia): Micromammals indicate a temperate and forest environment corresponding to GI-11 (MIS 3). Quat Sci Rev 229.

Argant A (1988) Etude de l'exemplaire de *Panthera spelaea* (Goldfuss, 1810) (Mammalia, Carnivora, Felidae) du gisement Pleistocéne moyen récent de la grotte d'Azé (Saône-et-Loire). Rev Paléobiol 7:449–466.

Argant A (1991) Carnivores quaternaires de Bourgogne. Documents des Laboratoires de Géologie de la Faculté des Sciences de Lyon 115:1–301.

Argant A, Argant J, Jeannet M, Erbajeva M (2007) The big cats of the fossil site Châteaux Breccia Northern Section (Saône-et-Loire, Burgundy, France): stratigraphy, palaeoenvironment, ethology and biochronological dating. Cour Forschungsinst Senckenberg 259:121–140.

Argant A (2010) Carnivores (Canidae, Felidae et Ursidae) de Romain-la-Roche (Doubs, France). Rev Paléobiolo 29:495–601.

Argant A, Brugal JP (2017) The cave lion *Panthera (Leo) spelaea* and its evolution: *Panthera spelaea intermedia* nov. subspecies. Acta Zool Cracov 60:59–104.

Ballesio R (1975) Étude de *Panthera (Leo) spelaea* (Goldfuss) nov. subsp. (Mammalia, Carnivora, Felidae) du gisement Pléistocène moyen des Abîmes de la Fage à Noailles (Corrèze). Nouv Arch Mus Hist Nat Lyon 13:47–55.

Ballesio R (1980) Le gisement pléistocène supérieur de la grotte de Jaurens à Nespouls, Corrèze, France: les carnivores (Mammalia, Carnivora). II Felidae. Nouv Arch Mus Hist Nat Lyon 18:61–102.

Barnett R, Shapiro B, Barnes I, Ho SY, Burger J, Yamaguchi N, Higham TF, Wheeler HT, Rosendahl W, Sher AV, Sotnikova M, Kuznetsova T, Baryshnikov GF, Martin LD, Harington CR, Burns JA, Cooper A (2009) Phylogeography of lions (*Panthera leo* ssp.) reveals three distinct taxa and a late Pleistocene reduction in genetic diversity. Mol Ecol 18:1668–77.

Barnett R, Zepeda Mendoza ML, Rodrigues Soares AE, Ho SYW, Zazula G, Yamaguchi N, Shapiro B, Kirillova IV, Larson G, Gilbert MTP (2016) Mitogenomics of the extinct cave lion, *Panthera spelaea* (Goldfuss, 1810), resolve its position within the Panthera cats. Open Quat 2:1–4.

Barycka E (2008) Middle and Late Pleistocene Felidae and Hyaenidae of Poland. Fauna Polski Museum and Institute of Zoology Polish Academy of Science, Warsaw, Poland.

Baryshnikov GF, Tsoukala E (2010) New analysis of the Pleistocene carnivores from Petralona cave (Macedonia, Greece) based on the collection of the Thessaloniki Aristotle University. Geobios 43:389–402.

Baryshnikov GF (2011) Pleistocene Felidae (Mammalia, Carnivora) from the Kudaro paleolithic cave sites in the Caucasus. Proc Zool Inst Russ Acad Sci 315:197–226.

Baryshnikov GF (2016) Late Pleistocene Felidae remains (Mammalia, Carnivora) from Geographical Society Cave in the Russian Far East. Proc Zool Inst RAS 320:84–120.

Bellani GG (2020) Zoogeography of felids. In: Bellani GG (ed) Felines of the World – Discoveries in Taxonomic Classification and History. Academic Press, pp 73–90.

Bergmann KGLC (1847) Über die Verhältnisse der wärmeokömie der Thiere zu ihrer. Göttinger Studien 3:595–708.

Binford LR (1981) Bones: Ancient Men and Modern Myths. New York, Academic Press.

Bishop MJ (1982) The mammal fauna of the early Middle Pleistocene cavern infill site of Westbury-sub-Mendip, Somerset. Spec Pap Palaeontol 28:1–108.

Bocherens H, Drucker DG, Bonjean D, Bridault A, Conard NJ, Cupillard C, Germonpré M, Honeisen M, Münzel SC, Napierrala H, Patou-Mathis M, Stephan E, Uerpmann HP, Ziegler R (2011) Isotopic evidence for dietary ecology of cave lion (*Panthera spelaea*) in North-western Europe: prey choice, competition and implications for extinction. Quat Int 245:249–261.

Bona F, Sardella R (2012) The middle Pleistocene large felids (Mammalia) from brecce di Soave (Verona, NE Italy). Riv Ital Paleontol Stratigr 118:193–199.

Bonifay MF (1971) Carnivores quaternaires du sudeest de la France. Mem Mus Hist Nat, série C 21:1–377.

Böse M, Lüthgens Ch, Lee JR, Rose J (2012) Quaternary glaciations of northern Europe. Quat Sci Rev 44:1–25.

Burger J, Rosendahl W, Loreille O, Hemmer H, Eriksson T, Götherström A, Hiller J, Collins MJ, Wess T, Alt KW (2004) Molecular phylogeny of the extinct cave lion *Panthera leo spelaea*. Mol Phylogenet Evol 30:841–849.

Caloi L, Palombo MR (1978) Anfibi, rettili e mammiferi di Torre del Pagliaccetto (Torre in Pietra, Roma). Quaternaria 20:315–428.

Candy I, Coope GR, Lee JR, Parfitt SA, Preece RC, Rose J, Schreve DC (2010) Pronounced warmth during early middle Pleistocene interglacials: investigating the mid-Brunhes event in the British terrestrial sequence. Earth Sci Rev 103:183–196.

Candy, I., Schreve, D.C., Sherriff, J. and Tye, G.J., 2014. Marine Isotope Stage 11: Palaeoclimates, palaeoenvironments and its role as an analogue for the current interglacial. Earth-Science Reviews, 128:18-51.

Christiansen P, Harris JM (2012) Variation in craniomandibular morphology and sexual dimorphism in pantherines and the saber cat *Smilodon fatalis*. PLoS One 7:e48352.

Crusafont-Pairó M, Casajuana MT (1950) Primer hallazgo del león de las cavernas, en el Pleistoceno de Catalunya. Pirineos 17–18:521–543.

deManuel M, Barnett R, Sandoval-Velasco M, Yamaguchi N, Vieira FG, Mendoza ML, Liu S, Martin MD, Sinding MH, Mak SS, Carøe C (2020) The evolutionary history of extinct and living lions. Proc Natl Acad Sci USA 117:10927–10934.

Diedrich, C.G., 2011. Late Pleistocene steppe lion *Panthera leo spelaea* (Goldfuss, 1810) footprints and bone records from open air sites in northern Germany–evidence of hyena-lion antagonism and scavenging in Europe. Quaternary Science Reviews, 30:1883-1906

Dietrich WO (1968) Fossile Löwen im Europäischen und afrikanischen Pleistozän. Paläont Abh Abt A 3:333–366.

Ehlers J, Grube A, Stephan HJ, Wansa S (2011) Pleistocene glaciations of North Germany – new results. In Ehlers J, Gibbard PL, Hugues PD (ed) Quaternary Glaciations – Extent and Chronology. A Closer Look. Developments in Quat Sci 15:149–162.

Elderfield H, Ferretti P, Greaves M, Crowhurst S, McCave I.N, Hodell D.A, Piotrowski A.M (2012) Evolution of Ocean Temperature and Ice Volume Through the Mid-Pleistocene Climate Transition. Science 337:704-709.

Filhol E, Filhol H (1871) Description des ossements de *Felis spelaea* decouverts dans la caverne de Lherm (Ariege). Ann Sci Nat Zool 14:1–120.

Garcia NG (2003) Osos y otros carnívoros de la Sierra de Atapuerca Fundacion oso de Asturias, dissertation Madrid.

Ghezzo E (2014) The Late Pleistocene site of Equi (Massa, Apuane Alps): revaluation of historical data and new discoveries. Morphological comparison of Italian and European felids. Dissertation, University of Florence.

Groiss J (1992) Neue Funde von quartären Grossäugern aus der Moggaster Höhle bei Ebermannstadt (Ofr.). Archaeopteryx 10:31–49.

Guérin C, Paupe P, Affolter J, Argant A, Argant J, Auguste P, Vercoutère C (2010) Le gisement pléistocène moyen récent de Romain-la-Roche (Doubs, France): Synthèse biostratigraphique et paléoécologique. Rev Paléobiol 29:881–895.

Hankó EP (2007) A revision of three Pleistocene subspecies of *Panthera*, based on mandible and teeth remains stored in Hungarian collections. Fragm Palaeontol Hung 24–25, 25–43.

Head MJ, Gibbard PL (2005) Early-Middle Pleistocene transitions: an overview and recommendation for the defining boundary. In: Head MJ, Gibbard PL (eds) Early-Middle Pleistocene Transitions: the Land-Ocean Evidence. Geological Society of London, Special Publication 247, pp 1–18.

Hemmer H (2004) Notes on the ecological role of European cats (Mammalia: Felidae) of the last two million years. Miscelanea en Homenaje a Emiliano Aquirre, Paleontologia 2:214–232.

Hemmer, H., Kahlke, R.D. and Vekua, A.K., 2001. The Jaguar-*Panthera onca gombaszoegensis* (Kretzoi, 1938) (Carnivora: Felidae) in the late lower pleistocene of Akhalkalaki (south Georgia; Transcaucasia) and its evolutionary and ecological significance. Geobios, 34:475-486.

Hemmer H, Schütt G (1970) Körpergrösse und extremitätenmasse Ältest und Altpleistozäner Europäischer Pantherkatzen (genus *Panthera*). Mz Naturw Arch 9:132-146.

Jansen JHF, Kuijpers A, Troelstra SR (1986) A mid-Brunhes climatic event: long-term changes in global atmosphere and ocean circulation. Science 232:619-622.

Kahlke RD (1999) The History of the Origin, Evolution and Dispersal of the Late Pleistocene *Mammuthus-Coelodonta* Faunal Complex in Eurasia (Large Mammals). Fenske Companies, Rapid City.

Kahlke RD, Garcia N, Kostopoulos DS, Lacombat F, Lister AM, Mazza PPA, Spassov N, Titov VV (2011) Western Palaearctic palaeoenvironment conditions during communities, and implications for hominin dispersal in Europe. Quat Sci Rev 30:1368–1395.

Kahlke RD (2014) The origin of Eurasian Mammoth Faunas (*Mammuthus-Coelodonta* Faunal complex). Quat Sci Rev 96:32-49.

Lewis M, Pacher M, Turner A (2010). The larger Carnivora of the West Runton freshwater bed. Quat Int 228:116–135.

Lindner L, Marks L, Nita M (2013) Climatostratigraphy of interglacials in Poland: middle and upper Pleistocene lower boundaries from a polish perspective. Quat Int 292:113–123.

Loarie SR, Tambling JC, Asner GP (2013) Lion hunting behaviour and vegetation structure in an African savanna. Anim Behav 85:899-906

López-García JM, Luzi E, Furió M, Susanna I, Llenas M, Madurell-Malapeira J (2016) Biochronological data for the Middle Pleistocene site of Grotte de la Carrière (Lachambre karstic complex, Corneilla-de-Conflent, eastern Pyrenees, southern France) inferred from the small-mammal assemblage. Quaternaire 27:133-138.

López-García JM, Cuenca-Bescós G, Galindo-Pellicena MÁ, Luzi E, Berto C, Lebreton L, Desclaux E (2021) Rodents as indicators of the climatic conditions during the Middle Pleistocene in the southwestern Mediterranean region: implications for the environment in which hominins lived. J Hum Evol 150:102911.

Madurell-Malapeira J, Ros-Montoya S, Espigares MP, Alba DM, Aurell-Garrido J (2014) Villafranchian large mammals from the Iberian Peninsula: paleobiogeography, paleoecology and dispersal events. J Iber Geol 40:167-178

Madurell-Malapeira J, Llenas M, Susanna I, Nebot M, Hernández T (2015) The paleontological sites of the Lachambre karstic complex (Rià and Cornellà de Conflent, Western Pyrenees). In: 1st International Convenion of Speleology (Barcelona, Spain, 2015).

Madurell-Malapeira J, Alba DM, Espigares MP, Vinuesa V, Palmqvist P, Martínez-Navarro B, Moyà-Solà S (2017) Were large carnivorans and great climatic shifts limiting factors for hominin dispersals? Evidence of the activity of *Pachycrocuta brevirostris* during the Mid-Pleistocene Revolution in the Vallparadís Section (Vallès-Penedès Basin, Iberian Peninsula). Quat Int 431:42–52.

Madurell-Malapeira J, Llenas M (2018) Projet de fouille programmée dans la Grotte de la Carrière. Corneillà de Conflent: Pyrénées-Orientales, Occitanie) (Unpublished Research Project).

Madurell-Malapeira J, Llenas M (2019) Projet de fouille programmée dans la Grotte de la Carrière. Corneillà de Conflent: Pyrénées-Orientales, Occitanie) (Unpublished Research Project).

Madurell-Malapeira J, Rufí I, Vinuesa V, Prat-Vericat M (2019) Réseau Lachambre : un complex de jaciments Pleistocens a la Vall del Têt (Pirineus Oriental, Occitània, França). Sedeck. Boletín de la Sociedad Española de Espeleología y Ciencias del Karst 14:44–55.

Marciszak A, Stefaniak K (2010) Two forms of cave lion: middle Pleistocene *Panthera spelaea fossilis* Reichenau, 1906 and upper Pleistocene *Panthera spelaea spelaea* Goldfuss, 1810 from the Bisnik cave, Poland. Neues Jahrb Geol Paläontol 258:339–351.

Marciszak A, Schouwenburg Ch, Darga R (2014) Decreasing size process in the cave (Pleistocene) lion *Panthera spelaea* (Goldfuss, 1810) evolution - a review. Quat Int 339–340:245–257.

Marciszak A, Gornig W, Stefaniak K (2017) Large mammals (carnivores, artiodactyls) from Solna Jama Cave (Bystrzyckie Mts, southwestern Poland) in the context of faunal changes in the postglacial period of central Europe. Palaeontol Electron 20:1–37.

Marciszak A, Lipecki G, Pawlowska K, Jakubowski G, Ratajczak-Skrzatek U, Zarzecka-Szubinska K, Nadachowski A (2021) The Pleistocene lion *Panthera spelaea* (Goldfuss, 1810) from Poland – A review. Quat Int 605:213–240.

Marciszak A, Schouwenburg C, Gorning W, Lipecki G, Mackiewicz P (2019) Morphometric comparison of *Panthera spelaea* (Goldfuss, 1810) from Poland with the lion remains from Eurasia over the last 700 ka. Quat Sci Rev 223:105950.

Moigne, A.M., Palombo, M.R., Belda, V., Heriech-Briki, D., Kacimi, S., Lacombat, F., de Lumley, M.A., Moutoussamy, J., Rivals, F., Quilčs, J. and Testu, A., 2006. Les faunes de grands mammifčres de la Caune de l'Arago (Tautavel) dans le cadre biochronologique des faunes du Pléistocčne moyen italien. L'anthropologie, 110:788-831.

Moore TY, Biewener AA (2015) Outrun or outmaneuver: predator–prey interactions as a model system for integrating biomechanical studies in a broader ecological and evolutionary context. Integr Comp Biol 55:1188-1197.

Musil R (1969) Eine karstspalte mit mittelpleistozänen Funden im Kalksteinbruch ˇZernavá. Casopis moravského musea. Védy prírodní 54:85–96.

Prat-Vericat M, Rufí I, Llenas M, Madurell-Malapeira J (2019) Úrsids del Pleistocè Mig i Superior de la Grotte de la Carrière (Pirineus Orientals, França). *Sedeck*. Boletín de la Sociedad Española de Espeleología y Ciencias del Karst 14, 44–55.

Prat-Vericat M, Rufí I, Llenas M, Madurell-Malapeira J (2020) Middle Pleistocene *Ursus deningeri* from Grotte de la Carrière (Réseau Lachambre, Têt Valley, Eastern Pyrenees). J Iber Geol 46:163–175.

Proctor CJ, Berridge PJ, Bishop MJ, Richards DA, Smart PL (2005) Age of middle Pleistocene fauna and lower Palaeolithic industries from Kent's cavern, Devon. Quat Sci Rev 24:1243–1252.

Rodríguez J, Alberdi MT, Azanza B, Prado JL (2004) Body size structure in north-western Mediterranean Plio-Pleistocene mammalian faunas. Global Ecol Biogeogr 13:163-176.

Sabol M (2011) Masters of the lost world: a hypothetical look at the temporal and spatial distribution of lion-like felids. Quaternaire, Horse-série 4:229–236.

Sabol M (2014) *Panthera fossilis* (Reichenau, 1906) (Felidae, Carnivora) from za Hájovnou cave (Moravia, the Czech Republic): a fossil record from 1987-2007. Acta Mus Nat Pragae Ser B His Nat 70:59–70.

Sabol M, Gullár J, Horvát J (2018) Montane record of the late Pleistocene *Panthera spelaea* (Goldfuss, 1810) from the Západné Tatry Mountains (northern Slovakia). J Vertebr Paleontol 38:e1467921.

Sala B (1990) *Panthera leo fossilis* (V. Reich., 1906) (Felidae) de Iserna la Pineta (Pléistocene moyen inférieur d'Italie). Geobios 23:189–194.

Schmid E (1940) Variations statistische Untersuchungen am Gebiß pleistozäner und rezenter Leoparden und anderer Feliden. Z Saugetierkd 15:1–179.

Schütt G (1969) Untersuchungen am Gebiß von *Panthera leo fossilis* (v. Reichenau, 1906) und *Panthera leo spelaea* (Goldfuss, 1810). Ein Beitrag zur Systematik der Pleistozänen Großkatzen Europas. Neues Jahrb Geol Paläontol 134:192–220.

Schütt G, Hemmer H (1978) Zur Evolution des Löwen (*Panthera leo* L.) im europäischen Pleistozän. Neues Jahrb Geol Paläontol Monatsh 4:228–255.

Sotnikova M, Nikolskiy P (2006) Systematic position of the cave lion *Panthera spelaea* (Goldfuss) based on cranial and dental characters. Quat Int 142–143:218–228.

Sotnikova MV, Foronova IV (2014) First Asian record of *Panthera* (leo) *fossilis* (Mammalia, Carnivora, Felidae) in the early Pleistocene of western Siberia, Russia. Integr Zool 9:517–530.

Stanton DWG, Alberti F, Plotnikov V, Androsov S, Grigoriev S, Fedorov S, Kosintsev P, Nagel D, Vartanyan S, Barnes I, Barnett R, Ersmark E, Döppes D, Germonpré M, Hofreiter M, Rosendahl W, Skoglund P, Dalén L (2021) Early Pleistocene origin and extensive intra-species diversity of the extinct cave lion. Sci Rep 10: 1–7.

Stuart AJ, Lister AM (2011) Extinction chronology of the cave lion *Panthera spelaea*. Quat Sci Rev 30:2329–2340.

Szymanek M, Julien MA (2018) Early and Middle Pleistocene climate-environment conditions in Central Europe and the hominin settlement record. Quat Sci Rev 198:56–75.

Terzea E (1965) *Panthera spelaea* Goldf. Pleistocenol superior din Romania. Lucraile Institutului de speologie Emil Rakovita 4:251–283.

Testu A (2006) Etude paléontologique et biostratigraphique des Felidae et Hyaenidae pléistocènes de l'Europe méditerranéenne. Dissertation, Faculté des Lettres et Sciences Humaines, Université de Perpignan.

Thenius E (1959) Die jungpleistozäne Wirbeltierfauna von Willendorf i. d. Wachau, NÖ. - Mitt prähist Komm Österr Akad Wiss 8/9:133–170.

Thenius E (1972) Die Feliden (Carnivora) aus dem Pleistozän von Stránská Skála. Anthropos 20:121–135.

Turner A (1984) Dental sex dimorphism in European lions (*Panthera leo* L.) of the Upper Pleistocene: palaeoecological and palaeoethological implications Ann Zool Fenn 21:1–8.

Turner A (2009) The evolution of the guild of large Carnivora of the British Isles during the middle and late Pleistocene. J Quat Sci 24:991–1005.

Van Valkenburgh B, Hayward MW, Ripple WJ, Meloro C, Roth VL (2016) The impact of large terrestrial carnivores on Pleistocene ecosystems. Proc Natl Acad Sci USA 113:862–867.

Werdelin L, Lewis ME (2005) Plio-Pleistocene Carnivora of eastern Africa: Species richness and turnover patterns. Zool J Linn Soc 144:121–144.

Zapfe H (1966) Die übrigen Carnivoren (außer Höhlenhyäne und Höhlenbär). Oesterr Akad Wiss Math-Naturwiss Kl, Denkschr 112:1–158.